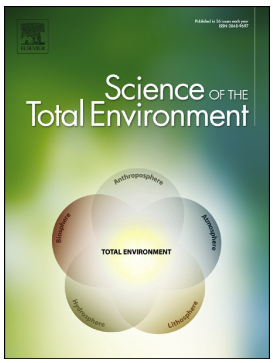


# A high-resolution record of Holocene primary productivity and water-column mixing from the varved sediments of Lake Żabińskie, Poland

Paul D. Zander, Maurycy Żarczyński, Hendrik Vogel, Wojciech Tylmann, Agnieszka Wacnik, Andrea Sanchini, Martin Grosjean

PII: S0048-9697(20)37244-2

DOI: https://doi.org/10.1016/j.scitotenv.2020.143713

Reference: STOTEN 143713

To appear in: *Science of the Total Environment*

Received date: 22 September 2020

Revised date: 9 November 2020

Accepted date: 9 November 2020

Please cite this article as: P.D. Zander, M. Żarczyński, H. Vogel, et al., A high-resolution record of Holocene primary productivity and water-column mixing from the varved sediments of Lake Żabińskie, Poland, *Science of the Total Environment* (2020), https://doi.org/10.1016/j.scitotenv.2020.143713

# A high-resolution record of Holocene primary productivity and water-column mixing from the varved sediments of Lake Żabińskie, Poland

Paul D. Zander[1*], Maurycy Żarczyński[2], Hendrik Vogel[3], Wojciech Tylmann[2], Agnieszka Wacnik[4], Andrea Sanchini[1], Martin Grosjean[1]

[1] *Institute of Geography & Oeschger Centre for Climate Change Research, University of Bern, Bern, Switzerland*

[2] *Faculty of Oceanography and Geography, University of Gdańsk, Poland*

[3] *Institute of Geological Sciences & Oeschger Centre for Climate Change Research, University of Bern, Bern, Switzerland*

[4] *W. Szafer Institute of Botany, Polish Academy of Sciences, Cracow, Poland*

[*] *Correspondence: E-mail address: paul.zander@giub.unibe.ch*

**Abstract**

Eutrophication and anoxia are increasing in lakes worldwide. However, our understanding of variations of primary productivity and anoxia in lakes over thousands of years is limited. Long-term records are needed to understand the natural variability of lake ecosystems, and to improve our understanding of drivers of productivity and anoxia. In this study, we used the varved sediment record of Lake Żabińskie, Poland to answer the following research questions: 1) How have primary production and water column oxygen concentrations varied during the past 10,800 years?; 2) What role did natural and anthropogenic forces have in driving changes in primary production or lake mixing regime? Recently developed hyperspectral imaging (HSI) techniques were used to quantify sedimentary chloropigments-*a* and bacteriopheopigments-*a* (Bphe-*a*) at sub-annual resolution. These data, combined with elemental data from micro X-ray fluorescence (μ-XRF) and pigment assemblage data from high-performance liquid chromatography (HPLC) measurements, were used to reconstruct paleolimnological conditions. Bphe-*a* was used as an indicator of anoxia, and its presence suggests that an extensive anoxic zone was present nearly continously from 10.8 to 2.8 ka BP. Anoxic conditions, driven by thermal stratification, were promoted by closed forest cover during that time, which limited wind-driven mixing of the water column. After 2.8 ka BP, water column oxygenation occurred more frequently, particularly during periods of increased human agricultural activity and forest opening. Pronounced anoxia was again present continuously from ~610-1470 CE, concurrent with a period of reforestation. After ~1610 CE, deforestation caused increases in erosion rates, algal production, and water column oxygenation. Pigment assemblages indicate that the algal community during the past 150 years was different from any other time during the Holocene. This study demonstrates a clear link between lake biogeochemical processes and forest cover and shows the potential of HSI to

produce extremely high-resolution records of past productivity and redox conditions from varved lake sediments.

Keywords: Hyperspectral imaging, Pigments, Varves, Anoxia, Eutrophication, Holocene

## 1. Introduction

Anthropogenic impacts to freshwater ecosystems have led to a global increase in eutrophication of lakes and increased occurrence and extent of anoxic or hypoxic zones (Carpenter, 2005; Friedrich et al., 2014; Jenny et al., 2016). These changes have primarily been attributed to higher nutrient loads and warmer summer temperatures that have, together, increased primary production in many lakes across a variety of ecosystems (Mills et al., 2017; Smith, 2003). Efforts to restore lake ecosystems have focused on nutrient reductions to slow eutrophication, however high primary production and hypoxia can persist for decades after management efforts are implemented (Jenny et al., 2016). Additionally, anthropogenic global warming is expected to increase anoxia in lakes because warmer temperatures enhance thermal stratification, which decreases oxygen transport to the hypolimnion, and warmer temperatures reduce oxygen solubility (Woolway and Merchant, 2019). To better understand the natural variability of lake ecosystems and the drivers controlling aquatic production and oxygenation, there is a need for long-term records of primary production and water column oxygen concentrations. Paleolimnological records can inform target conditions for restoration efforts and lake management (Bennion et al., 2011), and illuminate the sensitivity of lake ecosystems to forcing factors such as climate, land cover and land use, nutrient inputs and their combinations.

A variety of paleolimnological methods have been used to reconstruct past changes in lake trophic status and water column oxygen concentrations. Paleoproductivity has been reconstructed using changes in organic carbon (Meyers, 2006), C:N ratios, carbon and nitrogen stable isotopes (Schelske and Hodell, 1995; Talbot, 2005), assemblages of diatoms or other microfossils (Hall and Smol, 1999), pigments (Leavitt and Hodgson, 2002), and other sediment

variables. The majority of these methods require time-consuming laboratory analyses, which limits the resolution of paleoproductivity reconstructions over Holocene timescales. Past changes in oxygen concentration have been inferred from pigments and DNA associated with anoxygenic bacteria (Lotter, 2001; Sinninghe Damsté and Schouten, 2006; Wirth et al., 2013), and from microfossil assemblages (Clerk et al., 2000; Ursenbacher et al., 2020). Another approach is to use redox-sensitive elements such as Fe and Mn (Mackereth, 1966). This approach has become widely applied, in part because μ-XRF core scanners readily enable measurements of these elements at high resolution (Naeher et al., 2013; Wirth et al., 2013; Żarczyński et al., 2019). However, interpretation of these elements depends on site-specific characteristics and often requires complementary data from other sediment variables (Boyle, 2005; Davies et al., 2015). Due to these limitations, caveats should be considered when interpreting Fe and Mn as redox proxies (Naeher et al., 2013). The preservation of varves has also been used as an indicator of anoxic bottom-waters (Jenny et al., 2013; Zolitschka et al., 2015). Studies of sedimentary pigments have proven particularly useful for tracing changes in bacterial and algal communities, which can be used to reconstruct both productivity and oxygen concentrations. Conventional analyses of pigments are time-consuming and costly, leading to low-resolution reconstructions when applied to sediment records covering the Holocene or longer time-scales. Recently developed Hyperspectral Imaging (HSI) techniques enable rapid quantification of bulk pigment groups at sub-mm resolution (i.e. 60 x 60 μm pixel size) and these techniques have been used to investigate past lake productivity and oxygen concentrations at unprecedented temporal resolution (Butz et al., 2017, 2015; Gassner et al., 2020; Makri et al., 2020; Schneider et al., 2018; Tu et al., 2020).

Recent studies using HSI have demonstrated that land cover changes associated with Neolithic and Bronze Age agricultural development strongly influenced lake mixing regimes in small, relatively deep lakes (Gassner et al., 2020; Makri et al., 2020; Sanchini et al., 2020). However, less is known about the evolution of productivity and lake mixing in settings with minimal human impact throughout the Holocene. To investigate this question, we selected Lake Żabińskie in the Masurian Lakeland of northern Poland, where forest cover was not strongly modified by humans until ~1610 CE (Wacnik et al., 2016). Żarczyński et al. (2019) reconstructed major variations in bottom water oxygen at Lake Żabińskie during the past 2000 years based on Fe/Mn ratios and related these inferred mixing regime changes to changes in surrounding forest cover. In this study, we aimed to answer the following research questions: 1) How have primary production and water column oxygen concentrations varied during the past 10,800 years?; 2) What role did natural and anthropogenic forces have in driving changes in primary production or lake mixing regime? We hypothesized that land cover was the primary control on lake mixing throughout the Holocene. To investigate these research questions, we measured pigments in a long sediment core using Hyperspectral Imaging (HSI) and high-performance liquid chromatography (HPLC) and combined these with geochemical data (μ-XRF and CNS analysis). The Lake Żabińskie sediment record covers the past 10,800 years and is annually laminated throughout most of its length, making it an excellent archive to apply ultra-high-resolution scanning techniques. Calibrated HSI-inferred chloropigment and bacteriopheopigment concentrations enabled us to reconstruct past primary production and oxygen concentrations at sub-annual resolution.

## 2. Study Site

Lake Żabińskie is an eutrophic hard-water lake located in the post-glacial landscape of the Masurian Lakeland in northeastern Poland (54.1318° N, 21.9836° E; Fig. 1). The lake is a kettle-hole with a small surface area (41.6 ha) relative to its maximum depth (44.4 m), and a catchment area of 24.8 $km^2$. The catchment geology is dominated by glacial till, sandy moraines and fluvioglacial sands and gravels (Szumański, 2000). Land cover in the catchment is a mixture of agrarian and woodland areas (primarily oak-lime-hornbeam and pine forests; Wacnik et al., 2016). The lake has three inflows, including one from smaller Lake Purwin, and the outflow is a direct connection to much larger Lake Gołdopiwo. The site has been extensively studied for several years, with a focus on modern limnological and sedimentological processes, as well as multi-proxy investigations of the most recent 2000 years of the sediment record. Limnological monitoring showed inter-annual differences in the lake mixing regime with complete mixing occurring 0-2 times per year (Bonk et al., 2015a). Ice-cover typically lasts 2-4 months. Thermal stratification leads to anoxic conditions in the hypolimnion each summer. In some years the hypolimnion remains anoxic throughout the year, whereas in other years, mixing in the spring or fall brings oxygen into the bottom waters (Bonk et al., 2015a). The strong thermal stratification is attributed to the high relative depth of the lake (6.1 %; Wetzel et al., 1991) and steep basin morphology. Investigations of the sediment record identified major anthropogenic impacts starting in the 17$^{th}$ century, which led to increased catchment erosion, shifts in the algal communities, and eutrophication (Bonk et al., 2016; Hernández-Almeida et al., 2017). Żarczyński et al. (2019) showed that changes in bottom water oxygenation (inferred from Fe/Mn ratios) were caused by changes to the density of forest cover surrounding the lake.

## 3. Methods

Sediment cores were retrieved in 2012 using an UWITEC piston corer (ø90 mm), and surface cores were retrieved in 2017 using an UWITEC gravity corer (ø60 mm). Overlapping sections were visually correlated using distinctive stratigraphic layers to form a composite sequence of 19.4 m (Fig. S1). All depths mentioned in this study are composite depths below lake floor.

### *3.1 Geochronological methods*

The chronology presented here is a combination of previously published chronological data for the upper 13.1 m of the record and new chronological data for the section 19.4–13.1 m, which is published here for the first time (Fig. 2). The uppermost 6.3 m (corresponding to the last ~2000 years) was dated using varve counting as described in Żarczyński et al. (2018), and this chronology was transposed to our composite sequence. The reliability of the varve count was validated by radiocarbon ages (Bonk et al., 2015b; Żarczyński et al., 2018), $^{137}$Cs chronostratigraphic markers, a $^{210}$Pb profile, and identification of the 1875 CE Askja (Tylmann et al., 2016) and 860 CE White River Ash (Mount Churchill) tephras (Kinder et al., 2020). A mass movement deposit (MMD 2) from 7.3-6.3 m was removed from the chronology. The chronology from 13.1-7.3 m (~6.8-2.1 ka cal BP) was established by Zander et al. (2020), and is based on a V-sequence age model from the software OxCal (Bronk Ramsey, 2009, 2008; Bronk Ramsey and Lee, 2013), which combines age information from varve counts and radiocarbon ages.

The chronology for the remainder of the composite sequence is published here for the first time and is based primarily on radiocarbon ages. Eighteen samples of taxonomically identified

terrestrial plant macrofossils were measured for $^{14}C$ by AMS analysis at the University of Bern (Table S3). Detailed information about the radiocarbon sample preparation can be found in Zander et al., 2020. We used the age-depth modeling software OxCal (Bronk Ramsey, 2009, 2008; Bronk Ramsey and Lee, 2013) to generate an age-depth relation that links two P-sequences (16.4-13.1 m, and 19.4-18.0 m) with a V-sequence (17.0-16.4 m). MMD-1 (18.0-17.0 m) was excluded from age-depth modeling. The P-sequence is a Bayesian age-depth modeling routine that calibrates radiocarbon ages using IntCal13 (Reimer et al., 2013) and models sedimentation rates to fit the ages. Details about the chronologic methods can be found in the supplementary material (S1.1).

*3.2 Geochemical analyses*

µ-XRF scanning on the 2017 sediment-water interface cores (83-0 cm in our composite profile) was performed at the Swiss Federal Institute of Aquatic Science and Technology with an Avaatech XRF Core Scanner (Richter et al., 2006) equipped with a Rh-tube. Lighter elements were measured using 10 kv, 1.5 mA, and 15 s exposure time. Heavier elements (Cu, Zr) were measured using 40 kv, 2.0 mA, and 40 s exposure time. The scanning resolution was 0.5 mm. For the interval 2.5-2.1 m we used previously published µ-XRF data (Bonk et al., 2016; Żarczyński et al., 2019) to fill a gap where all core material had been sampled prior to scanning. These data were obtained using an ITRAX core scanner (Cox Analytical Systems) at the University of Bremen with a Mo-tube (exposure time 10 s, 30 kV, 18 mA), at a resolution of 0.2 mm. All other cores were scanned at the University of Bern using an ITRAX core scanner equipped with a Cr-tube (exposure time 20 s, 30 kV, 50 mA). The scanning resolution was 0.5 mm for 2.1-0.8 m and 2 mm resolution for 19.4 -2.5 m. All XRF data were calculated as counts

per second (cps) and then homogenized such that the standard deviation and mean for each element in overlapping core sections were equal. We selected key XRF elements for analysis based on data quality and interpretations of interest. Interpretations followed those of Davies et al. (2015) for XRF on lake sediments and previous work from the study site (Żarczyński et al., 2019). We used K, Zr and Ti as proxies for lithogenic input from the catchment; Fe, Mn, S and P as indicators of changing redox conditions; Cu and P as indicators of aquatic production or organic matter content, Ca/Ti ratio for endogenic calcite precipitation and Si/Ti ratio for biogenic silica (diatom and chrysophyte abundance).

Total inorganic carbon (TIC), total organic carbon (TOC), total nitrogen (TN), and total sulfur (TS) measurements for the interval 6.1-0 m were obtained at 3-year resolution, as reported in Żarczyński et al. (2019). For the interval 19.4-6.1 m these elements were measured at 10-cm resolution (1-cm-thick samples). TC, TN and TS were measured on these samples using a Vario El Cube elemental analyzer (Elementar). TIC was determined using loss-on-ignition at 950 °C (after samples were previously burned at 550 °C) (Heiri et al., 2001), and TOC was calculated by subtracting TIC from TC.

Dry bulk density (DBD) was measured on the same samples used for CNS analyses. Mass accumulation rates (MAR) were calculated by multiplying dry bulk density and sedimentation rate. Sedimentation rate was obtained from varve thickness over the section 13.1-0 m depth, and calculated from the OxCal age-depth model output for 19.4-13.1 m depth. To account for the variable measurement resolution of DBD, a LOESS regression was used to smooth the DBD data

prior to the MAR calculation. Fluxes were calculated by multiplying concentrations by MAR (a 60-year running mean was first applied to MAR for the sections with varve counts).

*3.3 Pigment analysis*

Pigment extractions were performed on 41 lyophilized samples weighing 0.2 to 0.6 g using 100% acetone, using a modified version of the method described in Amann et al. (2014). Samples were taken at ~500-year resolution for the period 10.8 to 2.0 ka cal BP and at ~100-year resolution from 2.0 ka cal BP to present. Extracts were measured using a spectrophotometer (Shimadzu UV-1800) for bulk concentrations of TChl-*a* (Total Chloropigments-*a*, defined as chlorophyll-*a* and chlorophyll derivatives-*a*) and Bphe-*a* (Bacteriopheopigments-*a*). We used the molar extinction coefficient for Bacteriopheophytin-*a* from Fiedor et al. (2002), and the molar extinction coefficient for chlorophyll-*a* and chlorophyll derivatives-*a* from Jeffrey and Humphrey (1975). The same pigment extracts were also analyzed using HPLC (Agilent Infinity 1260 series equipped with a G7117C Diode-Array Detection detector and a G7121A fluorescence detector) for specific pigment measurements following the procedures of Sanchini and Grosjean (2020). Sixteen pigment compounds were identified by comparisons to reference standards (Table S1). Two samples taken from within single varves were not considered for the pigment stratigraphy because the pigments represent seasonal deposition. The remaining 39 samples represent 2.5-23 years (mean = 8.5) of sedimentation per sample. All HPLC pigment concentrations were normalized to nmol per g of organic matter.

Hyperspectral imaging (HSI) was done using a Specim PFD-CL-65-V10E linescan camera following the methods of Butz et al. (2015). Relative absorption band depth (RABD) indices

were used to quantify absorption features associated with sedimentary pigments. Measurements were done at a resolution of 60 × 60 μm (pixel size). Details on the scanning methodology and index calculations can be found in the supplementary material. The $RABD_{655\text{-}685max}$ index represents TChl-*a* and is interpreted as representative of total algal abundance (Rein and Sirocko, 2002; Wolfe et al., 2006; Butz et al., 2017; Schneider et al., 2018). The $RABD_{845}$ index represents Bphe-*a*, a specific biomarker for purple sulfur bacteria (PSB). PSB live at the chemocline of stratified water bodies and require both light and reduced sulfur to photosynthesize (Van Gemerden and Mas, 1995). Therefore, the presence of Bphe-*a* indicates that the oxic/anoxic boundary was within the photic zone of the lake (Sinninghe Damsté and Schouten, 2006). Both RABD index values were calibrated to concentrations (μg/g dry sediments) via linear regression between the spectrophotometer measurements and the average RABD index values of the sample locations.

Interpretations of pigment taxonomic affiliations follow those of Bianchi and Canuel (2011), Guilizzoni and Lami (2003), Leavitt and Hodgson (2002), and Swain (1985). The CD/TC (Chlorophyll Derivatives/Total Carotenoids) ratio is used as an indicator of lake trophic state and/or preservation conditions because cyanobacteria produce more carotenoids than chloropigments, and carotenoids are better preserved under anoxic conditions (Swain, 1985). The Chlorophyll Preservation Index (CPI; (chlorophyll-*a*/(pheopigments-*a* + chlorophyll-*a*)) is an indicator of pigment preservation/degradation (Buchaca and Catalan, 2008). The ratio DDX+DT/Chl-*a* (DDX = Diadinoxanthin; DT = Diatoxanthin) is used as an indicator of light penetration (Hager, 1980; Riegman and Kraay, 2001).

*3.4 Pollen*

A 2000-year record of pollen from Żarczyński et al. (2019) was supplemented here with pollen samples targeting specific sediment sections with oxic/anoxic transitions to investigate the relationship between vegetation changes and shifts in lake mixing regime. We sampled four periods: 10,700-10,500 cal BP, 10,100-9600 cal BP, 7,700-7,400 cal BP, and 2,700-2,100 cal BP with 2-cm-thick samples (each sample represents 7-20 years). The methods of sample preparation and pollen counting are the same as in Żarczyński et al. (2019).

*3.5 Data Analysis*

Statistical analyses were conducted using R 3.6 (R Core Team, 2019). The packages 'ggplot2' (Wickham, 2016), 'factoextra' (Kassambara and Mundt, 2017), 'rioja' (Juggins, 2017), 'corrplot' (Wei and Simko, 2017) and 'zoo' (Zeileis and Grothendieck, 2005) were used for data analyses and visualization. Data from µ-XRF and HSI scanning and MARs were averaged to 1 cm resolution. Data from mass movement deposits or cracks were removed, and the data were log-transformed and scaled prior to statistical analyses. Principal component analysis (PCA) and an unconstrained cluster analysis were performed on this dataset to understand the relationships between different geochemical proxies and their variations over time. A broken-stick model was used to determine the number of significant principal components (Bennett, 1996). The cluster analysis was done using the kmeans method (1000 iterations). A stratigraphically constrained hierarchical cluster analysis (CONISS) was performed using 'rioja' (Juggins, 2017) for the HSI and µ-XRF dataset to identify geochemically similar stratigraphic units.

Statistical analysis of the HPLC pigment dataset was done separately. Pigment concentrations were square-root transformed and scaled prior to analysis. PCA and CONISS analyses were also

applied to the HPLC pigment data to identify zones of similar pigment assemblages and to aid interpretation. A broken-stick model was used to determine the number of zones in the pigment assemblage, as well as the number of significant principal components (Bennett, 1996).

## 4. Results and Interpretation

### *4.1 Core lithology and geochemical results*

The base of the 19.4-m-long sediment record was dated to 10,780 +102/-160 cal BP (Fig. 2). Details about chronological results are available in the supplementary material (S1.2). The sediments are generally composed of laminated (varved) carbonate- and organic-rich mud. Varves are preserved in approximately 16.2 m, representing ~93% of the record, excluding mass-movement deposits. Most varves consist of couplets of calcite-rich pale brown laminae (summer) and dark brown laminae composed of organic detritus and fine mineral matter (winter), though more complicated varve structures are also present. Żarczyński et al. (2018) presented detailed varve microfacies descriptions for the past 2000 years. Two mass movement deposits from 18.0-17.0 m and 7.3-6.3 m were identified by deformed laminae, massive beds, and fining-upwards sequences. We identified five lithotypes based on the results of the kmeans cluster analysis on HSI, XRF and MAR data (Fig. 3; Fig. 4). Example images of each lithotype and corresponding pigment maps from HSI are shown in Fig. 5.

Lithotype 1 (example image Fig. 5e) is defined by high MAR, Ca, and erosion indicators (Ti, K, Zr), whereas Fe, Mn, P and TChl-*a* are low. Sediments tend to be grayish in color, with relatively low TOC and high lithogenic content. Varve preservation ranges from good to absent; this lithotype represents more non-varved sediments than any other lithotype. Lithotype 1 primarily occurs from 10.8 to 10.3 ka cal BP, but is also identified occasionally throughout the record where more siliciclastic sediments occur. We interpret this lithotype as representative of periods with relatively high catchment erosion and low aquatic productivity. Bphe-*a* values vary across this lithotype, but are clearly high from 10.6 to 10.3 ka cal BP, indicating strongly anoxic

conditions, and this interpretation is supported by the presence of varves and low Fe and Mn in this period.

Lithotype 2 (example image Fig. 5d) is characterized by very high values of Fe and S, and very low TChl-*a* and Si. Erosional indicators and MAR are relatively low, whereas Bphe-*a* and Ca are relatively high. Sediments of this type are very dark, with the lowest light reflectance of any lithotype (Fig. S2). Varves are usually present, though faint at times, and there are some sections with disturbed varves or massive beds. This lithotype occurs almost exclusively in the interval 10.1-7.4 ka cal BP. We interpret this lithotype as representative of periods with low catchment erosion and low aquatic productivity. The formation of iron sulfides suggests that the hypolimnion was anoxic (Boyle, 2005), and Bphe-*a* concentrations above the detection limit confirm this.

Lithotype 3 (example image Fig. 5c) is the most common lithotype, and has very well-preserved varves with little variation in varve structure or thickness. Concentrations of TChl-*a* and Bphe-*a* are relatively high, as are Ca and P counts, whereas MAR, erosional indicators and Mn are low. Lithotype 3 is the dominant sediment type from 7.4 to 2.8 ka cal BP and from ~610 to 1610 CE. This lithotype is indicative of a strongly stratified water column and persistent hypolimnetic anoxia. Erosional input was relatively low, and aquatic production was relatively high.

Lithotype 4 (example image Fig. 5b) is characterized by high counts of Fe and Mn, high MAR, and low Bphe-*a* and erosional indicators. Sediments of this type show a more variable varve structure with reddish laminae rich in Fe and Mn present in many years. This lithotype is present

mainly from 2.8 to 1.3 ka cal BP. The high abundance of Mn implies that this lithotype represents periods when the lake mixed completely, and bottom waters were seasonally oxygenated.

Lithotype 5 (example image Fig. 5a) has a distinct geochemical signature with high or very high values of all considered elements except Ca and S. MAR is at maximum levels. TChl-*a* is highly variable, but reaches maximal concentrations in this lithotype, and fluxes of TChl-a are very high (Fig. S3). Bphe-*a* is very low in this lithotype. Varves are much thicker in this lithotype, with multiple calcite laminae visible in some years. This lithotype represents the most recent 300 years of sedimentation. This period is characterized by high erosional input from the catchment, high aquatic productivity, and complete seasonal mixing of the water column.

*4.2 Pigment analysis*

HSI pigment indices were calibrated and quantified using pigment concentrations measured by spectrophotometer. TChl-*a* was measured in 41 samples via spectrophotometer and these concentrations are significantly correlated with $RABD_{655\text{-}685max}$ ($r = 0.97$, $p<0.001$, RMSEP = 5.4%, Fig. S4). Bphe-*a* was detected in only 28 samples with the spectrophotometer, yet yields a significant correlation with $RABD_{845}$ ($r = 0.79$, $p<0.001$, RMSEP = 13.8%, Fig. S4). These correlations were confirmed by comparisons with HPLC data (Fig. S5). Bphe-*a* was measured in all samples by HPLC, and these measurements were used to estimate that the limit of detection for the $RABD_{845}$ index is ~0.992 (equivalent to approximately 5 $\mu g/g_{d.w.}$ Bphe-*a*).

The CONISS analysis on HPLC pigment data revealed four pigment zones (PZ; Fig. 6). The PCA analysis revealed two significant principal components (PCs). The first PC has positive loadings with all pigment compounds, and thus represents total pigment abundance, which is controlled by both lake productivity and pigment preservation. We interpret the second PC as indicative of community shifts between cyanobacteria (negative PC2 scores) and diatoms and chrysophytes (positive PC2 scores). This interpretation is based on negative PC2 loadings of canthaxanthin, echinenone, β,β-carotene, and {lutein + zeaxanthin} (these compounds were not separated chromatographically), and positive loadings of fucoxanthin, diatoxanthin, diadinoxanthin, and chlorophyll-*a*.

PZ-1 (Pigment Zone 1; 10.8-3.1 ka cal BP) represents the majority of the Holocene and is characterized by high concentrations of most pigments (high PC1 scores). A diverse and productive aquatic community is indicated by relatively high concentrations of β,β-carotene (total algal production), β,ε-carotene (cryptophytes and others), canthaxanthin (cyanobacteria), {lutein + zeaxanthin} (cyanobacteria/green algae), chlorophyll-*b* (green algae), and Bphe-*a* (PSB) (Bianchi and Canuel, 2011; Leavitt and Hodgson, 2002). Low PC2 scores and low CD/TC ratios (Swain, 1985) indicate cyanobacteria were relatively dominant in this zone.

PZ-2 (3.1-1.4 ka cal BP) is characterized by lower concentrations of most pigments. In particular, carotenoids such as {zeaxanthin + lutein} and echinenone reached their lowest values in this unit, and Bphe-*a* concentrations were very low. Low CPI values (Buchaca and Catalan, 2008) and higher CD/TC ratios (Swain, 1985), indicate that poor preservation may play a role in

lower pigment concentrations. PC2 scores are positive, suggesting a greater portion of the algal community was diatoms and/or chrysophytes, and cyanobacteria were less abundant.

PZ-3 (550-1800 CE) is characterized by an increase in pigment concentrations and abundant Bphe-*a*, suggesting anoxic conditions and increased pigment preservation. PC2 scores are high, indicating a similar algal assemblage to PZ-2 with diatoms and/or chrysophytes being relatively abundant, and cyanobacteria less abundant.

PZ-4 (1800 CE to present) contains the two most recent samples (dated ~1870 and 2009 CE), and has a unique pigment composition with a major increase in all pigment concentrations, except Bphe-*a*. Most pigments, particularly chlorophylls, reached their highest values in the sample from 1870 CE. However, canthaxanthin, echinone, {zeaxanthin + lutein}, β,β-carotene, and β,ε-carotene all increased between 1870 and 2009, most likely indicating a shift toward cyanobacteria.

*4.3 Paleolimnological reconstruction*

We divided the record into six phases (1-6) based on lithology and the results of a CONISS analysis on the HSI and XRF datasets (summarized in Table S2). Here we discuss the limnological conditions during each of those periods.

*Phase 1: 10.8-10.3 ka cal BP*

The basal age of the core (10,780 +102/-160 cal BP) represents a minimum age of lake formation. Deglaciation of the area occurred following the Pomeranian phase stadial of Vistulian

glaciation. Two cosmogenic $^{10}$Be ages from erratic boulders north and south of Lake Żabińskie suggest that the area was deglaciated between 14.51 ± 1.0 ka cal BP and 12.9 ± 1.0 ka cal BP (Rinterknecht et al., 2005). These findings suggest lake formation likely occurred prior to our basal age of 10.8 ka cal BP.

Phase 1 sediments are predominantly lithotype 1, indicating high erosion rates and anoxic conditions. Bphe-*a* was detectable in the oldest sediments, suggesting a deep, seasonally stratified lake with hypolimnetic anoxia in summer. Erosion rates were high initially (indicated by high Ti and MAR), but declined substantially by ~10,620 cal BP. From ~10,620 to 10,300 cal BP laminations were preserved, and Bphe-*a* and Fe/Mn increased, suggesting that lake mixing weakened even further, leading to prolonged periods of anoxia. When accounting for the high mass accumulation rates at that time, Bphe-*a* flux reached the highest value of the entire record at ~10,420 cal BP (Fig. 7). TChl-*a* concentrations were relatively low, but fluxes were relatively high.

The algal community in this phase featured a high abundance of cyanobacteria, as indicated by relatively high concentrations of canthaxanthin, echinenone, and {zeaxanthin + lutein} (see PZ-1, above). Productive conditions and seasonal stratification were likely influenced by strong seasonality with warm summer temperatures (Luoto et al., 2019; Street-Perrott et al., 2018; Tóth et al., 2015) and high P input from weakly developed soils on glacial drift (Boyle et al., 2015). The abundance of cyanobacteria may be an indication of N-limiting conditions (Smith, 1983). High productivity and high (but decreasing) erosional input during the early Holocene were also

found in several lakes in the Baltic region (Lauterbach et al., 2011; Street-Perrott et al., 2018; Wacnik, 2009a).

*Phase 2: 10.1-8.0 ka cal BP*

Phase 2 sediments are primarily lithotype 2, indicative of low erosional input and low productivity. Following the deposition of MMD-1 (mass movement deposit), anoxia quickly re-established, evidenced by good varve preservation and concentrations of Bphe-*a* above 10 $\mu g/g_{d.w.}$ within ~5 years after the mass movement event (Fig. S9). Lithogenic input was moderately high in the period following the event, but then decreased to very low values. Bphe-*a* concentrations peaked at ~9950 cal BP, and from ~10,060 cal BP until ~9,900 cal BP seasonal Bphe-*a* concentrations were below the detection limit in only six years. We interpret this period as a time of limited lake mixing, with most years not experiencing complete mixing.

From ~9,900 cal BP to ~8,800 cal BP, erosional input and concentrations of both TChl-*a* and Bphe-*a* decrease, while S and Fe counts are at their highest levels of the record. This suggests the presence of diagenetic iron sulfide formation, a clear indication that the sediments were anoxic and sulfidic during that time (Boyle, 2005). High sulfur concentrations were also found in Lake Łazduny (Sanchini et al., 2020) and Lake Suminko (Poland; Pedziszewska et al., 2015) during a similar time period, and in Lake Hańcza about 2000 years earlier (Lauterbach et al., 2011). The fact that high S deposition in the early Holocene is a common feature of these lakes suggests high S deposition may have been driven by sulfide oxidation in immature post-glacial soils. High availability of iron also enables sulfide formation (Boyle, 2005). Regional records report rising lake levels around 9,500 cal BP (Gałka et al., 2015; Pleskot et al., 2018), which could have

caused the depth of the chemocline to increase, leading to lower PSB production (light limitation) despite strong stratification and anoxic bottom-waters.

From ~8,800 cal BP to ~8,050 cal BP Bphe-*a* and TChl-*a* concentrations are very low; yet Bphe-*a* was still detectable, suggesting that the hypolimnion remained anoxic, at least seasonally. Sediments are rich in fine organic detritus and endogenic calcite, with little lithogenic input (low Ti). Low Bphe-*a* in this section could be explained by low productivity overall, which would limit oxygen consumption, possibly shrinking the extent of the anoxic zone.

HPLC pigment measurements in phase 2 show little change from phase 1, and are still classified as PZ-1. The CD/TC ratio was at the lowest level of the record, which is often associated with eutrophic conditions (Guilizzoni and Lami, 2003; Swain, 1985). However, low concentrations of TChl-*a* suggest productivity was not particularly high during this phase. We interpret the low CD/TC ratio as an indication of relative dominance of cyanobacteria, driven by N-limiting conditions that may have occurred due to minimal nutrient recycling in the lake during to stratified conditions and a lack of N-fixing vegetation in the catchment, particularly prior to the establishment of *Alnus* around 9.0 ka cal BP (Wacnik, 2009a)

*Phase 3: 8.0-2.8 ka cal BP*

This phase represents the majority of the record and is defined by moderately high TChl-*a* and Bphe-*a,* and very low Mn. This 6,200-year-long phase is characterized by anoxic and moderately productive conditions. The onset of the unit is defined by a drop in Fe and rise in P. Additionally, Ti counts increased at that time, associated with the deposition of several thin lithogenic beds

from ~8,050 cal BP to ~6,800 cal BP. Regional records of paleohydrology show conflicting results about whether this period was relatively wet (Dobrowolski et al., 2019; Wacnik, 2009b) or dry (Gałka et al., 2015; Gałka and Apolinarska, 2014; Pleskot et al., 2018). Lower lake levels would have exposed easily eroded shoreline sediments, possibly explaining the higher Ti counts. Alternatively, wetter conditions and increased runoff could have increased catchment erosion.

At ~7,540 cal BP concentrations of Bphe-*a* and TChl-*a* increased. The geochemical data shift from lithotype 2 to lithotype 3, indicating more anoxic and productive conditions. From 7.5 ka cal BP until 2.8 ka cal BP proxies indicate remarkably stable conditions with low erosional input, moderately high primary production, and a strongly stratified water column. A brief period around ~6,840 cal BP is the only major deviation from these stable conditions, with a short-term increase in erosional input and a shift towards more oxic conditions. Lake mixing was generally weak from 7.5 to 2.8 ka cal BP, though brief seasonal mixing events likely did occur to limit PSB production. A close-up figure demonstrates that PSB production was highly seasonal during that time (Fig. 5a). Anoxic conditions were also found in Lake Łazduny (Sanchini et al., 2020) and Tiefersee (northern Germany) during the mid-Holocene (Dräger et al., 2017).

The pigment assemblage remains classified as PZ-1, characterized by abundant cyanobacteria-related pigments. Maximal concentrations of β,β-carotene during this phase indicate that total algal productivity was high (Bianchi and Canuel, 2011).

*Phase 4: 2.8 ka cal BP – 610 CE*

Phase 4 is characterized by the presence of lithotype 4, which is indicative of more frequent complete mixing of the lake. Prior to the deposition of MMD-2 at ~2030 cal BP, lithotype 4 was interbedded with lithotype 3 sediments, and after MMD-2, lithotype 4 became the dominant lithotype. Low Bphe-*a* and spikes in Mn indicate major mixing events that were unprecedented in the record prior to this phase, with enough oxygen in the bottom waters to preserve Mn-oxides (Wirth et al., 2013; Żarczyński et al., 2019). Two periods of weakened mixing are indicated by peaks in Bphe-*a* from ~2,630 to ~2,520 cal BP and ~2,350 to ~2,200 cal BP.

HPLC measured pigments are classified as PZ-2, with generally lower concentrations, probably driven by reduced preservation associated with oxidation in the water column. This is reflected in relatively low CPI and CD/TC values (Buchaca and Catalan, 2008; Swain, 1985). Additionally, there is evidence (higher PC2 scores) of a shift from cyanobacteria to diatoms and/or chrysophytes.

*Phase 5: 610-1610 CE*

This phase is characterized by a return to lithotype 3 sediments and consistently high Bphe-*a* concentrations, indicating a strongly stratified water column and sustained anoxia overlapping with the photic zone. The transition to greater PSB production at ~610 CE occurred very rapidly. The seasonal maximum of Bphe-*a* increases from approximately 10 $\mu g/g_{d.w.}$ to a maximum of greater than 100 $\mu g/g_{d.w.}$ within 2 years (Fig. S7), suggesting a threshold effect occurred when anoxic and sulfidic conditions reached the photic zone of the lake. However, there are some indications that mixing was already weakening around ~550 CE, when Fe and Mn counts

declined, and iron-rich reddish laminae became less frequent, suggesting that oxygenation of the bottom-waters was becoming less frequent. Bphe-*a* was also detected more frequently from ~530-610 CE compared to the previous four centuries. From ~610 to ~1470 CE, only 30 varves contained Bphe-*a* concentrations below the detection limit, suggesting that the lake was likely meromictic for the majority of this period. Interestingly, the Fe/Mn ratio (along with P counts) increased approximately 100 years after Bphe-*a* increased, possibly because of delayed development of Fe and P saturation in the hypolimnion (Boehrer et al., 2017). Fe/Mn ratios stayed high throughout the remainder of the meromictic period. Ca/Ti ratios and % TIC declined throughout this phase, likely driven by depletion of $Ca^{2+}$ ions in the epilimnion and/or dissolution of calcite in the cold, low-pH, hypolimnion (Hernández-Almeida et al., 2014; Wetzel, 2001). This dissolution would have strengthened the density gradient between hypolimnion and epilimnion and further limited water column mixing. This anoxic period is well-described by Żarczyński et al., (2019) and is associated with a period of reduced human activity and reforestation, as recorded by maximum tree pollen percentages (Fig. 8). The timing of this anoxic period is roughly similar to a period of anoxia in Tiefersee (Dräger et al., 2017), and maximum Bphe-*a* production in Lake Łazduny (Sanchini et al., 2020; Fig. 7).

After ~1470 CE, Bphe-*a* concentrations dropped below the detection limit with increasing frequency, indicating brief seasonal mixing events. From ~1560 to ~1610 CE, Bphe-*a* concentrations were consistently near or below the detection limit, and decreasing Fe/Mn ratios confirm greater oxygenation of the hypolimnion.

The pigment stratigraphy during this phase is classified as PZ-3 and shows improved preservation (higher CPI values) associated with more anoxic conditions. Assemblages remained similar to the previous phase with relatively high abundances of diatoms and chrysophytes.

*Phase 6: 1610 to 2017 CE*

The most recent sediments of Lake Żabińskie are mainly lithotype 5, characterized by very high MAR, high counts of erosion indicators Ti, K, Zr, and high TChl-*a* flux. These data, together, indicate major erosional input from the catchment and a shift towards more eutrophic conditions. These changes were associated with major deforestation and intensified agricultural land use surrounding the lake (Fig. 7; Wacnik et al., 2016, Żarczyński et al., 2019). Bphe-*a* concentrations were near or below the detection limit in this phase and Mn counts reached high levels, indicating strengthened seasonal mixing and oxygenation of the hypolimnion.

Two pigment samples were measured in this zone, from ~1870 and 2009 CE, and these samples contain the highest concentrations of most pigments, showing a clear anthropogenic eutrophication effect as has been observed in numerous European lakes (Guilizzoni et al., 2002; Sanchini et al., 2020; Schneider et al., 2018b; Tõnno et al., 2019). Canthaxanthin, echinone, zeaxanthin, lutein, β,β-carotene, and β,ε-carotene were relatively low in the sample from ~1870 CE and increased greatly in the sample from 2009 CE, indicating a community shift towards cyanobacteria. This shift toward cyanobacteria dominance was found in a previous pigment study from Lake Żabińskie focused on the past century (Amann et al., 2014) and has been observed in lakes across the northern hemisphere (Taranu et al., 2015).

## 5. Discussion

### *5.1 Holocene aquatic productivity*

Models of nutrient flux from catchment soils to lakes in postglacial landscapes suggest that P fluxes are greatest immediately after deglaciation, and decline exponentially over time (Boyle, 2007; Boyle et al., 2015). High TChl-*a* flux (Fig. S3) and high concentrations of carotenoids (Fig. 5) during phase 1 of the Lake Żabińskie record (10.8-10.3 ka cal BP) support this notion. However, TChl-*a* flux reached minimum values between 9.0 and 7.0 ka cal BP and then slowly increased to moderately high values from 3.0 ka cal BP to ~1600 CE. In contrast to the HSI-inferred TChl-*a* record, TC concentrations and CD/TC ratios, which have often been used as indicators of trophic levels (Guilizzoni et al., 2011; Guilizzoni and Lami, 2003; Swain, 1985), suggest more eutrophic conditions prior to 3.3 ka cal BP, and less eutrophic conditions from 2.8 to 0.3 ka cal BP. These discrepancies may be explained by three possible factors: 1) sedimentary carotenoid concentrations are influenced by preservation conditions and anoxia in addition to trophic state (Leavitt and Hodgson, 2002; Swain, 1985); 2) TChl-*a* measurements from HSI may underestimate TChl-*a* concentrations in very dark sediments that occur from 9.9 to 7.5 ka cal BP; 3) nitrogen-limiting conditions may have promoted cyanobacteria dominance (Smith, 1983), particularly during the early Holocene, prior to the establishment of N-fixing plants, such as *Alnus* (established approximately 9.0 ka cal BP; Wacnik, 2009a).

Several records in the region confirm an increasing trend in aquatic productivity during the Holocene, for instance, pigments from Lake Łazduny (30 km south of Lake Żabińskie, Sanchini et al., 2020; Fig. 7) and Lake Peipsi (Estonia, Tõnno et al., 2019), and biogenic silica data from Lake Suminko (northern Poland, Pedziszewska et al., 2015). Principal component analysis of

pigment assemblages from Lake Łazduny revealed broadly similar Holocene trends in pigment assemblages as the Lake Żabińskie record (PC1 of each site is plotted in Fig. 7, see also Fig. S8), suggesting the patterns seen in Lake Żabińskie may be regionally representative for lakes with similar properties (i.e. small, relatively deep lakes). The trend towards higher productivity over the Holocene in several lakes suggests that ontogenetic processes led to natural eutrophication in these lakes (Fritz and Anderson, 2013). In contrast to the gradual ontogenetic increase in productivity, the effect of cultural eutrophication on Lake Żabińskie was sudden and severe. After ~1720 CE, TChl-*a* flux increased by 300% (Fig. 7), and the most recent two HPLC samples from ~1870 and 2009 CE show much higher pigment concentrations than all previous samples, with PC1 scores clearly outside the range of past natural variability. A similar result was obtained from Lake Łazduny pigment data (Fig. 7, Fig. S8).

*5.2 Drivers of lake mixing regime*

Lake stratification is influenced by a number of factors, such as exposure to wind, summer temperatures, aquatic production, and others (Boehrer and Schultze, 2008). Based on previous work using Fe/Mn ratios to trace oxygenation of Lake Żabińskie during the past 2000 years (Żarczyński et al., 2019), we hypothesized that vegetative cover was the primary controlling factor of the mixing regime at Lake Żabińskie during the Holocene. Dense forest cover shelters the lake from wind, reducing vertical mixing of the water column. Fig. 7 compares the record of anoxia (as indicated by Bphe-*a* flux) in Lake Żabińskie with regional reconstructions of lake productivity, vegetation and temperature. Anoxic phases (high Bphe-*a*) occurred during the warm middle Holocene but also during cooler times in the early Holocene and during the past 2000 years. Anoxic phases tended to occur during times with higher algal production (indicated

by TChl-*a* flux), but the relationship did not always hold, for instance during the period from ~1 to 600 CE. The more consistent driver of anoxia appears to be forest cover. Anoxic periods were associated with times of high tree pollen %, while periods with lower tree pollen were associated with greater oxygenation (low Bphe-*a*).

We investigated the relationship between lake stratification and forest cover more closely through selected case studies of periods when the mixing regime changed (Fig. 8, Fig. S9). The earliest phase of very high Bphe-*a* flux (~10,620-10,380 cal BP) occurred during a time when tree pollen (TP) represented more than 94% of pollen counts (Fig. S9). The pollen assemblage was dominated by *Pinus sylvestris* (up to 87%) and *Betula* (up to 22%), indicating that the lake was surrounded by pine dominated forests and pine-birch communities, probably with a greater share of birch on the lake shoreline. This forest, composed of tall trees species, would have shielded the small lake from wind, leading to meromixis.

Annual temperatures at that time were likely cooler than modern, but relatively warm in the summer; a pattern that is driven by the lingering Fennoscandian ice sheet (Stroeven et al., 2016) and high summer insolation (Laskar et al., 2004). Temperature reconstructions from pollen in the Baltic region (Sweden, Finland, Estonia, Latvia) suggest annual temperatures around 10.5 ka cal BP were 2-4 °C cooler than modern conditions, but similar to modern during summer months (Heikkilä and Seppä, 2010; Holmström et al., 2015). Chironomid-based summer temperature reconstructions from Żabieniec peat-bog in central Poland place summer temperatures close to modern values (Kotrys et al., 2019). Warm summers and cold winters create a favorable situation

for meromictic conditions because there is less time during the year when the surface waters can be 4-5 °C, the temperature required for the lake to fully mix.

From ~10,000 to ~9,850 cal BP, Bphe-*a* concentrations declined substantially, and TP % decreased from 83% to 51% (Fig. 8a, Fig. S9). This regional shift in vegetation was driven mainly by *Corylus avellana* expansion and was accompanied by decreasing *Betula* and *Ulmus* after ~9,830 cal BP (Fig. S9). The formation of a scrub woodland dominated by hazel near the lake would have allowed more wind shear on the lake surface. Several brief peaks in Bphe-*a* between 9,900 and 9,700 cal BP are associated with short-term increases in TP (Fig. 8a), suggesting that lake mixing and plant cover were linked at decadal timescales. The long-term declining trend in Bphe-*a* continued until approximately 8.0 ka cal BP. This period of low Bphe-*a* corresponds with lower % arboreal pollen recorded in the Lake Łazduny sediment record from 8.9 to 7.8 ka cal BP (Fig. 7), providing further evidence that enhanced lake mixing, caused by increased wind shear, could have limited PSB production and that this was a regional phenomenon.

A shift toward strengthened stratification and more anoxic conditions occurred at ~7,540 cal BP. A slight shift toward more tree pollen also occurred at that time; however, inter-sample variability was high (Fig. 8b). Short-term increases in Bphe-*a* appear to track peaks in % TP between ~7,530 and ~7,460 cal BP, suggesting that the lake mixing regime was sensitive to decadal-scale variations in forest cover.

Proxy data indicate relatively little change in lake mixing regime from 7.5 to 2.8 ka cal BP. Stable, stratified, anoxic conditions promoted growth of PSB. Although the first cereal pollen are recorded in the region around 5,700 cal BP during the Neolithic period, forest cover was not significantly modified by humans at that time (Wacnik, 2009b). Pollen data from Lake Łazduny (Sanchini et al., 2020) and Lake Miłkowskie (Wacnik, 2009a, 2009b) indicate generally stable and closed forest cover until the middle Bronze Age around 3.4-3.0 ka cal BP. After ~3.4 ka cal BP, agriculture became increasingly important for the economy of local human communities (Wacnik et al., 2012). Changes to forest cover at that time were local and impermanent. Nonetheless, declines in shares of arboreal taxa such as *Corylus*, *Tilia*, *Carpinus*, and *Picea* and increases of light-demanding *Betula* and herbaceous plants show that the forest cover was reduced via small clearings (Wacnik et al., 2012). These changes appear to have affected the mixing regime of Lake Żabińskie, as indicated by declining Bphe-*a* from ~2,960 to ~2,810 cal BP. Forest opening likely led to increased wind shear on the surface of the lake, leading to increased mixing. Pollen counts of cultivated species from Lake Żabińskie confirm human modification of forest cover near the lake by ~2,730 cal BP (Fig. S9; no samples were analyzed for pollen from 7.3 to 2.8 ka cal BP, so cultivation may have begun earlier).

A high-resolution pollen dataset for the past two millennia (Żarczyński et al., 2019) enabled a close investigation of the link between lake mixing and forest cover (Fig. 8c, 8d). Between ~1 CE and ~540 CE, forest cover was relatively dense (average TP % = 89%). However, the presence of cultivated plants (Fig. 7) and charred microparticles provide clear evidence of human impacts to vegetation (Żarczyński et al., 2019). Bphe-*a* was consistently near or below the detection limit during that time, indicating complete mixing of the lake. Between ~540 and ~610

CE, TP increased from 88% to 97%, and the percentage of cultivated plant pollen declined. Simultaneously, geochemical indicators suggest the lake was mixing less frequently (Fig. 8c). Meromictic conditions likely persisted from ~610 to ~1470 CE. During that time TP averaged 96%, and cultivated plant pollen averaged 0.2%. From ~1470 to ~1590 CE, TP declines slightly to 93% and cultivated plant pollen increases to 1.0%. These subtle changes led to a gradual decline in PSB production, with Bphe-*a* concentrations reaching the detection limit in several years, however PSB were clearly present until ~1560 CE, indicating stratified and anoxic conditions.

The percentage of TP decreased rapidly after ~1610 CE, reaching values as low as 53% by ~1870 CE. This strong deforestation of the lake catchment area caused major increases in erosion, and algal production, leading to a major increase in sedimentation rates. Low Fe/Mn ratios and Bphe-*a* concentrations below the detection limit during the past few centuries indicate that seasonal mixing was complete in most years.

In the decades following the Second World War, forests in the Masurian Lakeland have expanded (Wacnik et al., 2012), and this was true around Lake Żabińskie as well (Wacnik et al., 2016). Tree pollen averaged 86% from 1995 to 2010 CE, and a slight increase in Bphe-*a* is visible in the HSI data after ~2000 CE (Fig. 8c), but values are still near the detection limit. HPLC measurements also show a slight increase in Bphe-*a* in the most recent sample from 2009 CE compared to samples from ~1870 and ~1730 CE. This evidence, along with increased S concentrations, likely indicate a return to more stratified or anoxic conditions in the past few decades caused by recent afforestation. Limnologic conditions are, however, fundamentally

different from conditions prior to human impacts (Hernández-Almeida et al., 2017) and may react to forcing differently. In particular, light penetration is restricted now because of higher epilimnetic productivity, and this may explain the low Bphe-*a* concentrations in the most recent sediments (Fig. 5a), despite stratified and anoxic conditions persisting throughout much of the year in modern limnological measurements (Bonk et al., 2015a). Evidence of light limitation for PSB is seen in the seasonal timing of Bphe-*a* in recent years (Bphe is low during spring/summer, and higher during fall/winter; Fig. 5a).

Comparisons of the Holocene Bphe-*a* record and vegetation reconstructions point to forest cover as the most important factor controlling stratification of Lake Żabińskie. Fig. 8d demonstrates the non-linear relationship between forest cover and Bphe-*a* production, whereby Bphe-*a* concentrations increase dramatically when TP is greater than ~90%. We summarize the occurrence of strongly stratified and anoxic conditions by observing the % of 3-year periods with average Bphe-*a* concentrations above the detection limit (5 $\mu g/g_{d.w.}$). Prior to 2.8 ka, when forests in the region experienced no, or weak, human impacts (Karpińska-Kołaczek et al., 2014; Sanchini et al., 2020; Wacnik, 2009a), Bphe-*a* was present 97% of the time. From 2.8 ka cal BP to ~610 CE, when localized forest clearing for cultivation occurred (Wacnik, 2009b; Wacnik et al., 2012; Żarczyński et al., 2019), Bphe-*a* was present in only 23% of 3-year periods. During a period of reforestation from ~610 to ~1610 CE (Żarczyński et al., 2019), Bphe-*a* was present again 95% of the time. Since ~1720 CE, after extensive deforestation (Wacnik et al., 2016; Żarczyński et al., 2019), there have been no 3-year periods with average Bphe-*a* concentrations above the detection limit. A relationship between forest cover and lake mixing has been observed in several small, deep lakes in Europe such as Tiefersee in northern Gemany (Dräger et al.,

2017), Lake Łazduny in Poland (Sanchini et al., 2020), Soppensee (Lotter, 2001) and Moossee (Makri et al., 2020) in Switzerland, and Lake Zazari in Greece (Gassner et al., 2020). All of these lakes experienced stratified, anoxic conditions prior to large-scale forest clearing for agricultural expansion (Neolithic, Bronze Age or historic times).

Despite the clear importance of vegetation in controlling lake mixing, climate and lake productivity also likely influence the extent and persistence of anoxia. Low PSB production from 9.5 to 7.4 ka cal BP may have been influenced by low aquatic productivity overall. Additionally, summer temperatures may also be an important driver of lake stratification. In Lake Żabińskie, the prolonged period of high PSB production from 7.4 to 2.8 ka cal BP coincided with maximal Holocene temperatures (Fig. 7), and the shift towards more oxic conditions at 2.8 ka cal BP occurred during a grand solar minimum with relatively cool temperatures (Davis et al., 2003; Steinhilber et al., 2009). Additionally, oxic conditions during phase 4 (2.8 ka cal BP – 610 CE) and anoxic conditions during phase 5 (610-1610 CE) coincided with relatively cool and warm periods, respectively (Dobrowolski et al., 2019; Luterbacher et al., 2016). However, highly resolved local temperature data are lacking prior to 1000 CE. During the last millennium, summer and winter temperature reconstructions from Lake Żabińskie based on chironomids and chrysophytes, respectively, show little relation to variations of Bphe-*a* (Hernández-Almeida et al., 2017). In all likelihood, prolonged stratification of Lake Żabińskie is only possible when minimum levels of summer warmth, primary production and forest density are exceeded.

*5.3 Methodological advantages*

The combination of high-resolution scanning techniques (μ-XRF and HSI) on varved sediments with specific HPLC pigment analysis enabled us to infer changes in past environmental conditions at unprecedented high temporal resolution and obtain detailed information about algal communities. HPLC measurements confirmed our interpretations and calibrations of the RABD indices to pigment concentrations (Fig. S6), which is critical for remotely sensed HSI data (Butz et al., 2015; Schneider et al., 2018). We also used HPLC measurements of Bphe-*a* to estimate the limit of detection of Bphe-*a* with the HSI method. This information is essential for interpretation of the HSI record of Bphe-*a*. HPLC techniques enabled us to measure specific pigment compounds that cannot be detected by HSI. By differentiating the chloropigments that make up the bulk absorption band $RABD_{655\text{-}685max}$, we gain insights about pigment preservation, light penetration, and organic matter cycling in the lake (e.g. CPI index, Buchaca and Catalan, 2008; Sanchini and Grosjean, 2020). Specific carotenoid pigments provide information about algal assemblages, making it possible to recognize the important role of cyanobacteria in lake productivity, whereas cyanobacteria are under-represented in the $RABD_{655\text{-}685max}$ index because of their lower chlorophyll production (Amann et al., 2014; Swain, 1985). Low (DDX+DT)/Chl-*a* ratios are indicative of reduced light penetration (Buchaca and Catalan, 2008; Hager, 1980; Riegman and Kraay, 2001). The fact that these ratios are low when Bphe-*a* is highest from ~610-1470 CE provides confirming evidence that PSB production was not driven by improved light penetration, but rather by more anoxic conditions.

Our HSI technique records seasonal-scale variations of Bphe-*a* and TChl-*a* deposition, enabling us to track changing aquatic conditions with unprecedented detail. For instance, we observed a

10-fold increase in seasonal Bphe-*a* concentration within 2 years at ~610 CE (Fig. S7). There is no visible change in lithology when the first blooms of PSB occur, so this observation is only made possible by the HSI technique. The HSI data also enabled investigation of the seasonal cycle of Bphe-*a* and TChl-*a* deposition. We find that seasonal maxima of Bphe-*a* typically occur simultaneously with maxima of TChl-*a* (Fig. 5c, d, e; Fig. S7). Both pigment groups usually peak immediately below (prior to) white calcite layers, indicating maximum PSB and phytoplankton production occurred in spring or early summer. However, during the most recent ~25 years, Bphe-*a* peaks were offset from TChl-*a* peaks and occur after calcite precipitation (Fig. 5a). This pattern is likely explained by reduced light availability caused by eutrophication in modern times. Suitable conditions for PSB now only occur during late summer when epilimnetic production is limited by low nutrient concentrations under strong lake stratification (Bonk et al., 2015a). An additional benefit of the HSI technique is that HSI measurements of TChl-*a* appear to be less affected by preservation problems than HPLC measurements of specific pigments.

## 6. Conclusions and outlook

The use of hyperspectral imaging to quantify pigments in the varved sedimentary record of Lake Żabińskie enabled us to reconstruct changes in algal productivity and lake mixing at sub-annual resolution throughout the past 10,800 years. The combination of high-resolution, non-specific pigment measurements with low-resolution ,specific HPLC measurements strengthens our interpretation of the record. Bacteriopheopigments were used as an indicator of purple sulfur bacteria, which are indicative of anoxic conditions within the photic zone. We find that anoxia and a stratified water column persisted through the majority of the Holocene. Prior to 2.8 ka cal

BP, Bphe-*a* concentrations were above the detection limit in ~97% of 3-year averages. After 2.8 ka cal BP the lake mixing regime alternated between periods of enhanced mixing and periods of strengthened stratification. Permanent anoxia and high PSB production persisted from ~610 to 1470 CE, concurrent with a reforestation period. During the past few centuries, forest clearing and increased agricultural land use have led to greater algal production, but also greater oxygenation of the water column. Through comparisons with other proxy data from our site and the region, we investigated how external drivers impact lake productivity and mixing regime. We found that the primary control on lake mixing is the density of forest cover surrounding the lake. However, temperature (mainly in summer) and lake productivity could also influence the extent and persistence of anoxia. We showed evidence of linkages between forest cover and lake mixing related to both anthropogenic (Bronze Age and later) and natural vegetation changes (Early and Middle Holocene). Changes to lake mixing occurred simultaneously with changes in forest cover.

This study shows the potential of HSI studies on sediment cores for inferring past environmental change at sub-annual resolution. Future studies can utilize this approach to investigate rates of change, regime shifts, and other questions that require datasets with very high resolution. We advocate for application of HSI pigment measurements in combination with HPLC techniques for long-term paleolimnological studies to understand short-term variability in limnological conditions and to gain a more complete understanding of changes in aquatic ecosystems and their catchments.

## Data Availability

Data produced for this project will be made publicly available at the Bern Open Repository and Information System (DOI: 10.7892/boris.147848).

## Acknowledgements

This project was funded by Swiss National Science Foundation grant 200021_172586, and Polish National Science Centre grant 2014/13/B/ST10/01311. The work of AW was additionally supported by the Statutory Research Tasks of the W. Szafer Institute of Botany (PAS). We thank Sönke Szidat, Gary Salazar, Edith Vogel, Ron Lloren, Irene Brunner, Stamatina Makri, Linus Rösler, Petra Boltshauser-Kaltenrieder, and Daniela Fisher for their contributions to this study. PZ and MG designed the study. PZ did primary laboratory analyses and data analysis. HV and PZ did µ-XRF scanning. AW did pollen and charcoal analysis. AS assisted with pigment analysis and interpretation. WT and MZ provided core material and data. PZ wrote the manuscript with contributions from all authors. We thank Mark Brenner and an anonymous reviewer for their thoughtful comments.

**References**

Amann, B., Lobsiger, S., Fischer, D., Tylmann, W., Bonk, A., Filipiak, J., Grosjean, M., 2014. Spring temperature variability and eutrophication history inferred from sedimentary pigments in the varved sediments of Lake Żabińskie, north-eastern Poland, AD 1907-2008. Glob. Planet. Change 123, 86–96. https://doi.org/10.1016/j.gloplacha.2014.10.008

Bennett, K.D., 1996. Determination of the number of zones in a biostratigraphical sequence. New Phytol. 132, 155–170. https://doi.org/10.1111/j.1469-8137.1996.tb04521.x

Bennion, H., Battarbee, R.W., Sayer, C.D., Simpson, G.L., Davidson, T.A., 2011. Defining reference conditions and restoration targets for lake ecosystems using palaeolimnology: A synthesis. J. Paleolimnol. 45, 533–544. https://doi.org/10.1007/s10933-010-9419-3

Bianchi, T.S., Canuel, E.A., 2011. Chemical biomarkers in aquatic ecosystems. Princeton University Press.

Boehrer, B., Schultze, M., 2008. Stratification of lakes. Rev. Geophys. 46, 1–27. https://doi.org/10.1029/2006RG000210

Boehrer, B., von Rohden, C., Schultze, M., 2017. Physical Features of Meromictic Lakes: Stratification and Circulation, in: Gulati, R.D., Zadereev, E.S., Degermendzhi, A.G. (Eds.), Ecology of Meromictic Lakes. Springer International Publishing, pp. 15–34. https://doi.org/10.1007/978-3-319-49143-1_2

Bonk, A., Kinder, M., Enters, D., Grosjean, M., Meyer-Jacob, C., Tylmann, W., 2016. Sedimentological and geochemical responses of Lake Żabińskie (north-eastern Poland) to erosion changes during the last millennium. J. Paleolimnol. 56, 239–252. https://doi.org/10.1007/s10933-016-9910-6

Bonk, A., Tylmann, W., Amann, B., Enters, D., Grosjean, M., 2015a. Modern limnology and

varve-formation processes in lake Żabińskie, northeastern Poland: Comprehensive process studies as a key to understand the sediment record. J. Limnol. 74, 358–370. https://doi.org/10.4081/jlimnol.2014.1117

Bonk, A., Tylmann, W., Goslar, T., Wacnik, A., Grosjean, M., 2015b. Comparing varve counting and 14C-Ams chronologies in the sediments of Lake Żabińskie, Northeastern Poland: Implications for accurate 14C dating of lake sediments. Geochronometria 42, 157–171. https://doi.org/10.1515/geochr-2015-0019

Boyle, J.F., 2007. Loss of apatite caused irreversible early-Holocene lake acidification. Holocene. https://doi.org/10.1177/0959683607077046

Boyle, J.F., 2005. Inorganic Geochemical Methods in Paleolimnology, in: Tracking Environmental Change Using Lake Sediments. Kluwer Academic Publishers, pp. 83–141. https://doi.org/10.1007/0-306-47670-3_5

Boyle, J.F., Chiverrell, R.C., Davies, H., Alderson, D.M., 2015. An approach to modelling the impact of prehistoric farming on Holocene landscape phosphorus dynamics. Holocene. https://doi.org/10.1177/0959683614556381

Bronk Ramsey, C., 2009. Bayesian Analysis of Radiocarbon Dates. Radiocarbon 51, 337–360. https://doi.org/10.1017/s0033822200033865

Bronk Ramsey, C., 2008. Deposition models for chronological records. Quat. Sci. Rev. 27, 42–60. https://doi.org/10.1016/j.quascirev.2007.01.019

Bronk Ramsey, C., Lee, S., 2013. Recent and Planned Developments of the Program OxCal. Radiocarbon 55, 720–730. https://doi.org/10.1017/s0033822200057878

Buchaca, T., Catalan, J., 2008. On the contribution of phytoplankton and benthic biofilms to the sediment record of marker pigments in high mountain lakes. J. Paleolimnol. 40, 369–383.

https://doi.org/10.1007/s10933-007-9167-1

Butz, C., Grosjean, M., Fischer, D., Wunderle, S., Tylmann, W., Rein, B., 2015. Hyperspectral imaging spectroscopy: a promising method for the biogeochemical analysis of lake sediments. J. Appl. Remote Sens. 9, 096031. https://doi.org/10.1117/1.jrs.9.096031

Butz, C., Grosjean, M., Goslar, T., Tylmann, W., 2017. Hyperspectral imaging of sedimentary bacterial pigments: a 1700-year history of meromixis from varved Lake Jaczno, northeast Poland. J. Paleolimnol. 58, 57–72. https://doi.org/10.1007/s10933-017-9955-1

Carpenter, S.R., 2005. Eutrophication of aquatic ecosystems: Bistability and soil phosphorus. Proc. Natl. Acad. Sci. U. S. A. 102, 10002–10005. https://doi.org/10.1073/pnas.0503959102

Clerk, S., Hall, R., Quinlan, R., Smol, J.P., 2000. Quantitative inferences of past hypolimnetic anoxia and nutrient levels from a Canadian Precambrian Shield lake. J. Paleolimnol. 23, 319–336. https://doi.org/10.1023/A:1008147127606

Davies, S.J., Lamb, H.F., Roberts, S.J., 2015. Micro-XRF Core Scanning in Palaeolimnology: Recent Developments. https://doi.org/10.1007/978-94-017-9849-5_7

Davis, B.A.S., Brewer, S., Stevenson, A.C., et al., 2003. The temperature of Europe during the Holocene reconstructed from pollen data. Quat. Sci. Rev. 22, 1701–1716. https://doi.org/10.1016/S0277-3791(03)00173-2

Dobrowolski, R., Mazurek, M., Osadowski, Z., Alexandrowicz, W.P., Pidek, I.A., Pazdur, A., Piotrowska, N., Drzymulska, D., Urban, D., 2019. Holocene environmental changes in northern Poland recorded in alkaline spring-fed fen deposits – A multi-proxy approach. Quat. Sci. Rev. 219, 236–262. https://doi.org/10.1016/j.quascirev.2019.05.027

Dräger, N., Theuerkauf, M., Szeroczyńska, K., Wulf, S., Tjallingii, R., Plessen, B., Kienel, U., Brauer, A., 2017. Varve microfacies and varve preservation record of climate change and

human impact for the last 6000 years at Lake Tiefer See (NE Germany). Holocene 27, 450–464. https://doi.org/10.1177/0959683616660173

Fiedor, J., Fiedor, L., Kammhuber, N., Scherz, A., Scheer, H., 2002. Photodynamics of the Bacteriochlorophyll–Carotenoid System. 2. Influence of Central Metal, Solvent and β-Carotene on Photobleaching of Bacteriochlorophyll Derivatives. Photochem. Photobiol. 76, 145. https://doi.org/10.1562/0031-8655(2002)0760145POTBCS2.0.CO2

Friedrich, J., Janssen, F., Aleynik, D., et al., 2014. Investigating hypoxia in aquatic environments: Diverse approaches to addressing a complex phenomenon. Biogeosciences 11, 1215–1259. https://doi.org/10.5194/bg-11-1215-2014

Fritz, S.C., Anderson, N.J., 2013. The relative influences of climate and catchment processes on Holocene lake development in glaciated regions. J. Paleolimnol. 49, 349–362. https://doi.org/10.1007/s10933-013-9684-z

Gałka, M., Apolinarska, K., 2014. Climate change, vegetation development, and lake level fluctuations in Lake Purwin (NE Poland) during the last 8600 cal. BP based on a high-resolution plant macrofossil record and stable isotope data (δ13C and δ18O). Quat. Int. 328–329, 213–225. https://doi.org/10.1016/j.quaint.2013.12.030

Gałka, M., Tobolski, K., Rubak, I., 2015. Late Glacial and Early Holocene lake level fluctuations in NE Poland tracked by macro-fossil, pollen and diatom records. Quat. Int. 388, 23–38. https://doi.org/10.1016/j.quaint.2014.03.009

Gassner, S., Gobet, E., Schwörer, C., et al., 2020. 20,000 years of interactions between climate, vegetation and land use in Northern Greece. Veg. Hist. Archaeobot. https://doi.org/10.1007/s00334-019-00734-5

Guilizzoni, P., Lami, A., 2003. Paleolimnology: Use of Algal Pigments as Indicators, in:

Encyclopedia of Environmental Microbiology. John Wiley & Sons, Inc. https://doi.org/10.1002/0471263397.env313

Guilizzoni, P., Lami, A., Marchetto, A., Jones, V., Manca, M., Bettinetti, R., 2002. Palaeoproductivity and environmental changes during the Holocene in central Italy as recorded in two crater lakes (Albano and Nemi). Quat. Int. 88, 57–68. https://doi.org/10.1016/S1040-6182(01)00073-8

Guilizzoni, P., Marchetto, A., Lami, A., Gerli, S., Musazzi, S., 2011. Use of sedimentary pigments to infer past phosphorus concentration in lakes. J. Paleolimnol. 45, 433–445. https://doi.org/10.1007/s10933-010-9421-9

Hall, R.I., Smol, J.P., 1999. Diatoms as indicators of lake eutrophication, in: Stoermer, E.F., Smol, J.P. (Eds.), The Diatoms: Applications for the Environmental and Earth Sciences, Second Edition. Cambridge University Press, Cambridge, UK, pp. 128–168. https://doi.org/10.1017/CBO9780511763175.008

Heikkilä, M., Seppä, H., 2010. Holocene climate dynamics in Latvia, eastern Baltic region: A pollen-based summer temperature reconstruction and regional comparison. Boreas 39, 705–719. https://doi.org/10.1111/j.1502-3885.2010.00164.x

Heiri, O., Lotter, A.F., Lemcke, G., 2001. Loss on ignition as a method for estimating organic and carbonate content in sediments: Reproducibility and comparability of results. J. Paleolimnol. https://doi.org/10.1023/A:1008119611481

Hernández-Almeida, I., Grosjean, M., Gómez-Navarro, J.J., et al., 2017. Resilience, rapid transitions and regime shifts: Fingerprinting the responses of Lake Żabińskie (NE Poland) to climate variability and human disturbance since AD 1000. Holocene 27, 258–270. https://doi.org/10.1177/0959683616658529

Hernández-Almeida, I., Grosjean, M., Tylmann, W., Bonk, A., 2014. Chrysophyte cyst-inferred variability of warm season lake water chemistry and climate in northern Poland: training set and downcore reconstruction. J. Paleolimnol. 53, 123–138. https://doi.org/10.1007/s10933-014-9812-4

Holmström, L., Ilvonen, L., Seppä, H., Veski, S., 2015. A Bayesian spatiotemporal model for reconstructing climate from multiple pollen records. Ann. Appl. Stat. 9, 1194–1225. https://doi.org/10.1214/15-AOAS832

Jeffrey, S.W., Humphrey, G.F., 1975. New spectrophotometric equations for determining chlorophylls a, b, c1 and c2 in higher plants, algae and natural phytoplankton. Biochem. und Physiol. der Pflanz. https://doi.org/10.1016/s0015-3796(17)30778-3

Jenny, J.P., Arnaud, F., Dorioz, J.M., et al., 2013. A spatiotemporal investigation of varved sediments highlights the dynamics of hypolimnetic hypoxia in a large hard-water lake over the last 150 years. Limnol. Oceanogr. 58, 1395–1408. https://doi.org/10.4319/lo.2013.58.4.1395

Jenny, J.P., Francus, P., Normandeau, A., Lapointe, F., Perga, M.E., Ojala, A., Schimmelmann, A., Zolitschka, B., 2016. Global spread of hypoxia in freshwater ecosystems during the last three centuries is caused by rising local human pressure. Glob. Chang. Biol. 22, 1481–1489. https://doi.org/10.1111/gcb.13193

Juggins, S., 2017. rioja: Analysis of Quaternary Science Data, R package version (0.9-21).

Karpińska-Kołaczek, M., Kołaczek, P., Stachowicz-Rybka, R., 2014. Pathways of woodland succession under low human impact during the last 13,000 years in northeastern Poland. Quat. Int. 328–329, 196–212. https://doi.org/10.1016/j.quaint.2013.11.038

Kassambara, A., Mundt, F., 2017. factoextra: Extract and Visualize the Results of Multivariate

Data Analyses. R package version 1.0.5.

Kinder, M., Wulf, S., Appelt, O., Hardiman, M., Żarczyński, M., Tylmann, W., 2020. Late-Holocene ultra-distal cryptotephra discoveries in varved sediments of Lake Żabińskie, NE Poland. J. Volcanol. Geotherm. Res. 402, 106988. https://doi.org/10.1016/j.jvolgeores.2020.106988

Kotrys, B., Płóciennik, M., Sydor, P., Brooks, S.J., 2019. Expanding the Swiss-Norwegian chironomid training set with Polish data. Boreas. https://doi.org/10.1111/bor.12406

Laskar, J., Robutel, P., Joutel, F., Gastineau, M., Correia, A.C.M., Levrard, B., 2004. A long-term numerical solution for the insolation quantities of the Earth. Astron. Astrophys. 428, 261–285. https://doi.org/10.1051/0004-6361:20041335

Lauterbach, S., Brauer, A., Andersen, N., et al., 2011. Multi-proxy evidence for early to mid-Holocene environmental and climatic changes in northeastern Poland. Boreas 40, 57–72. https://doi.org/10.1111/j.1502-3885.2010.00159.x

Leavitt, P.R., Hodgson, D.A., 2002. Sedimentary Pigments, in: Tracking Environmental Change Using Lake Sediments. Springer, Dordrecht, pp. 295–325. https://doi.org/10.1007/0-306-47668-1_15

Lotter, A.F., 2001. The palaeolimnology of Soppensee (Central Switzerland), as evidenced by diatom, pollen, and fossil-pigment analyses. J. Paleolimnol. 25, 65–79. https://doi.org/10.1023/A:1008140122230

Luoto, T.P., Kotrys, B., Płóciennik, M., 2019. East European chironomid-based calibration model for past summer temperature reconstructions. Clim. Res. 77, 63–76. https://doi.org/10.3354/cr01543

Luterbacher, J., Werner, J.P., Smerdon, J.E., et al., 2016. European summer temperatures since

Roman times. Environ. Res. Lett. https://doi.org/10.1088/1748-9326/11/2/024001

Mackereth, F.J.H., 1966. Some chemical observations on post-glacial lake sediments. Philos. Trans. R. Soc. Lond. B. Biol. Sci. 250, 165–213. https://doi.org/10.1098/rstb.1966.0001

Makri, S., Rey, F., Gobet, E., Gilli, A., Tinner, W., Grosjean, M., 2020. Early human impact in a 15,000-year high-resolution hyperspectral imaging record of paleoproduction and anoxia from a varved lake in Switzerland. Quat. Sci. Rev. 239, 106335. https://doi.org/10.1016/j.quascirev.2020.106335

Meyers, P.A., 2006. An Overview of sediment organic matter records of human eutrophication in the Laurentian Great Lakes region, in: The Interactions Between Sediments and Water. Springer Netherlands, pp. 89–99. https://doi.org/10.1007/978-1-4020-5478-5_10

Mills, K., Schillereff, D., Saulnier-Talbot, É., et al., 2017. Deciphering long-term records of natural variability and human impacts recorded in lake sediments: a palaeolimnological puzzle. Wiley Interdiscip. Rev. Water 4, e1195. https://doi.org/10.1002/wat2.1195

Naeher, S., Gilli, A., North, R.P., Hamann, Y., Schubert, C.J., 2013. Tracing bottom water oxygenation with sedimentary Mn/Fe ratios in Lake Zurich, Switzerland. Chem. Geol. 352, 125–133. https://doi.org/10.1016/j.chemgeo.2013.06.006

Pedziszewska, A., Tylmann, W., Witak, M., Piotrowska, N., Maciejewska, E., Latałowa, M., 2015. Holocene environmental changes reflected by pollen, diatoms, and geochemistry of annually laminated sediments of Lake Suminko in the Kashubian Lake District (N Poland). Rev. Palaeobot. Palynol. 216, 55–75. https://doi.org/10.1016/j.revpalbo.2015.01.008

Pleskot, K., Tjallingii, R., Makohonienko, M., Nowaczyk, N., Szczuciński, W., 2018. Holocene paleohydrological reconstruction of Lake Strzeszyńskie (western Poland) and its implications for the central European climatic transition zone. J. Paleolimnol. 59, 443–459.

https://doi.org/10.1007/s10933-017-9999-2

R Core Team, 2019. R: A Language and Environment for Statistical Computing. Vienna, Austria.

Rein, B., Sirocko, F., 2002. In-situ reflectance spectroscopy - Analysing techniques for high-resolution pigment logging in sediment cores. Int. J. Earth Sci. 91, 950–954. https://doi.org/10.1007/s00531-002-0264-0

Richter, T.O., Van Der Gaast, S., Koster, B., Vaars, A., Gieles, R., De Stigter, H.C., De Haas, H., Van Weering, T.C.E., 2006. The Avaatech XRF Core Scanner: Technical description and applications to NE Atlantic sediments. Geol. Soc. Spec. Publ. 267, 39–50. https://doi.org/10.1144/GSL.SP.2006.267.01.03

Rinterknecht, V.R., Marks, L., Piotrowski, J.A., Raisbeck, G.M., Yiou, F., Brook, E.J., Clark, P.U., 2005. Cosmogenic 10Be ages on the Pomeranian Moraine, Poland. Boreas. https://doi.org/10.1111/j.1502-3885.2005.tb01014.x

Sanchini, A., Grosjean, M., 2020. Quantification of chlorophyll a, chlorophyll b and pheopigments a in lake sediments through deconvolution of bulk UV–VIS absorption spectra. J. Paleolimnol. 0123456789. https://doi.org/10.1007/s10933-020-00135-z

Sanchini, A., Szidat, S., Tylmann, W., Vogel, H., Wacnik, A., Grosjean, M., 2020. A Holocene high-resolution record of aquatic productivity, seasonal anoxia and meromixis from varved sediments of Lake Łazduny, North-Eastern Poland: insight from a novel multi-proxy approach. J. Quat. Sci.

Schelske, C.L., Hodell, D.A., 1995. Using carbon isotopes of bulk sedimentary organic matter to reconstruct the history of nutrient loading and eutrophication in Lake Erie. Limnol. Oceanogr. 40, 918–929. https://doi.org/10.4319/lo.1995.40.5.0918

Schneider, T., Rimer, D., Butz, C., Grosjean, M., 2018. A high-resolution pigment and productivity record from the varved Ponte Tresa basin (Lake Lugano, Switzerland) since 1919: insight from an approach that combines hyperspectral imaging and high-performance liquid chromatography. J. Paleolimnol. 60, 381–398. https://doi.org/10.1007/s10933-018-0028-x

Seppä, H., Poska, A., 2004. Holocene annual mean temperature changes in Estonia and their relationship to solar insolation and atmospheric circulation patterns. Quat. Res. 61, 22–31. https://doi.org/10.1016/j.yqres.2003.08.005

Sinninghe Damsté, J.S., Schouten, S., 2006. Biological markers for anoxia in the photic zone of the water column. Handb. Environ. Chem. Vol. 2 Reactive Process. 2 N, 127–163. https://doi.org/10.1007/698_2_005

Smith, V.H., 2003. Eutrophication of freshwater and coastal marine ecosystems: A global problem. Environ. Sci. Pollut. Res. https://doi.org/10.1065/espr2002.12.142

Smith, V.H., 1983. Low nitrogen to phosphorus ratios favor dominance by blue-green algae in lake phytoplankton. Science (80-. ). 221, 669–671. https://doi.org/10.1126/science.221.4611.669

Steinhilber, F., Beer, J., Fröhlich, C., 2009. Total solar irradiance during the Holocene. Geophys. Res. Lett. 36, 1–5. https://doi.org/10.1029/2009GL040142

Street-Perrott, F.A., Holmes, J.A., Robertson, I., Ficken, K.J., Koff, T., Loader, N.J., Marshall, J.D., Martma, T., 2018. The Holocene isotopic record of aquatic cellulose from Lake Äntu Sinijärv, Estonia: Influence of changing climate and organic-matter sources. Quat. Sci. Rev. 193, 68–83. https://doi.org/10.1016/j.quascirev.2018.05.010

Stroeven, A.P., Hättestrand, C., Kleman, J., et al., 2016. Deglaciation of Fennoscandia. Quat.

Sci. Rev. https://doi.org/10.1016/j.quascirev.2015.09.016

Swain, E.B., 1985. Measurement and interpretation of sedimentary pigments. Freshw. Biol. 15, 53–75. https://doi.org/10.1111/j.1365-2427.1985.tb00696.x

Szumański, A., 2000. Objaśnienia do Szczegółowej Mapy Geologicznej Polski, Arkusz Giżycko, (Explanation to the Detailed Geological Map of Poland, Sheet Gizycko (104)). Warsaw, Poland.

Talbot, M.R., 2005. Nitrogen Isotopes in Palaeolimnology, in: Tracking Environmental Change Using Lake Sediments. Kluwer Academic Publishers, pp. 401–439. https://doi.org/10.1007/0-306-47670-3_15

Taranu, Z.E., Gregory-Eaves, I., Leavitt, P.R., et al., 2015. Acceleration of cyanobacterial dominance in north temperate-subarctic lakes during the Anthropocene. Ecol. Lett. 18, 375–384. https://doi.org/10.1111/ele.12420

Tõnno, I., Nauts, K., Belle, S., Nõmm, M., Freiberg, R., Kõiv, T., Alliksaar, T., 2019. Holocene shifts in the primary producer community of large, shallow European Lake Peipsi, inferred from sediment pigment analysis. J. Paleolimnol. 61, 403–417. https://doi.org/10.1007/s10933-019-00067-3

Tóth, M., Magyari, E.K., Buczkó, K., Braun, M., Panagiotopoulos, K., Heiri, O., 2015. Chironomid-inferred Holocene temperature changes in the South Carpathians (Romania). Holocene 25, 569–582. https://doi.org/10.1177/0959683614565953

Tu, L., Zander, P., Szidat, S., Lloren, R., Grosjean, M., 2020. The influences of historic lake trophy and mixing regime changes on long-term phosphorus fractions retention in sediments of deep, eutrophic lakes: a case study from Lake Burgäschi, Switzerland. Biogeosciences 17, 2715–2729. https://doi.org/10.5194/bg-2019-389

Tylmann, W., Bonk, A., Goslar, T., Wulf, S., Grosjean, M., 2016. Calibrating 210 Pb dating results with varve chronology and independent chronostratigraphic markers: Problems and implications. Quat. Geochronol. 32, 1–10. https://doi.org/10.1016/j.quageo.2015.11.004

Ursenbacher, S., Stötter, T., Heiri, O., 2020. Chitinous aquatic invertebrate assemblages in Quaternary lake sediments as indicators of past deepwater oxygen concentration. Quat. Sci. Rev. 231, 106203. https://doi.org/10.1016/j.quascirev.2020.106203

Van Gemerden, H., Mas, J., 1995. Ecology of phototrophic sulfur bacteria, in: Anoxygenic Photosynthetic Bacteria. Springer, Dordrecht, pp. 49–85. https://doi.org/10.1007/0-306-47954-0

Wacnik, A., 2009a. Vegetation development in the Lake Miłkowskie area, north-eastern Poland, from the Plenivistulian to the late Holocene. Acta Palaeobot. 49, 287–335.

Wacnik, A., 2009b. From foraging to farming in the Great Mazurian Lake District: Palynological studies on Lake Miłkowskie sediments, northeast Poland. Veg. Hist. Archaeobot. 18, 187–203. https://doi.org/10.1007/s00334-008-0196-0

Wacnik, A., Goslar, T., Czernik, J., 2012. Vegetation changes caused by agricultural societies in the Great Mazurian Lake District. Acta Palaeobot. 52, 59–104.

Wacnik, A., Tylmann, W., Bonk, A., Goslar, T., Enters, D., Meyer-Jacob, C., Grosjean, M., 2016. Determining the responses of vegetation to natural processes and human impacts in north-eastern Poland during the last millennium: combined pollen, geochemical and historical data. Veg. Hist. Archaeobot. 25, 479–498. https://doi.org/10.1007/s00334-016-0565-z

Wei, T., Simko, V., 2017. R package "corrplot": Visualization of a Correlation Matrix.

Wetzel, R.G., 2001. Limnology: Lake and River Ecosystems, third ed. Academic Press, San

Diego, CA, USA. https://doi.org/10.1046/j.1529-8817.2001.37602.x

Wetzel, R.G., Likens, G.E., Wetzel, R.G., Likens, G.E., 1991. Lake Basin Characteristics and Morphometry, in: Limnological Analyses. Springer New York, pp. 1–14. https://doi.org/10.1007/978-1-4757-4098-1_1

Wickham, H., 2016. ggplot2: Elegant Graphics for Data Analysis.

Wirth, S.B., Gilli, A., Niemann, H., et al., 2013. Combining sedimentological, trace metal (Mn, Mo) and molecular evidence for reconstructing past water-column redox conditions: The example of meromictic Lake Cadagno (Swiss Alps). Geochim. Cosmochim. Acta 120, 220–238. https://doi.org/10.1016/j.gca.2013.06.017

Wolfe, A.P., Vinebrooke, R.D., Michelutti, N., Rivard, B., Das, B., 2006. Experimental calibration of lake-sediment spectral reflectance to chlorophyll a concentrations: Methodology and paleolimnological validation. J. Paleolimnol. https://doi.org/10.1007/s10933-006-9006-6

Woolway, R.I., Merchant, C.J., 2019. Worldwide alteration of lake mixing regimes in response to climate change. Nat. Geosci. 12, 271–276. https://doi.org/10.1038/s41561-019-0322-x

Zander, P.D., Szidat, S., Kaufman, D.S., Żarczyński, M., Poraj-Górska, A.I., Boltshauser-Kaltenrieder, P., Grosjean, M., 2020. Miniature radiocarbon measurements (< 150µgC) from sediments of Lake Żabińskie, Poland: effect of precision and dating density on age–depth models. Geochronology 2, 63–79. https://doi.org/10.5194/gchron-2-63-2020

Żarczyński, M., Tylmann, W., Goslar, T., 2018. Multiple varve chronologies for the last 2000 years from the sediments of Lake Żabińskie (northeastern Poland) – Comparison of strategies for varve counting and uncertainty estimations. Quat. Geochronol. 47, 107–119. https://doi.org/10.1016/j.quageo.2018.06.001

Żarczyński, M., Wacnik, A., Tylmann, W., 2019. Tracing lake mixing and oxygenation regime using the Fe/Mn ratio in varved sediments: 2000 year-long record of human-induced changes from Lake Żabińskie (NE Poland). Sci. Total Environ. 657, 585–596. https://doi.org/10.1016/j.scitotenv.2018.12.078

Zeileis, A., Grothendieck, G., 2005. Zoo: S3 infrastructure for regular and irregular time series. J. Stat. Softw. https://doi.org/10.18637/jss.v014.i06

Zolitschka, B., Francus, P., Ojala, A.E.K., Schimmelmann, A., 2015. Varves in lake sediments - a review. Quat. Sci. Rev. 117, 1–41. https://doi.org/10.1016/j.quascirev.2015.03.019

## Figures

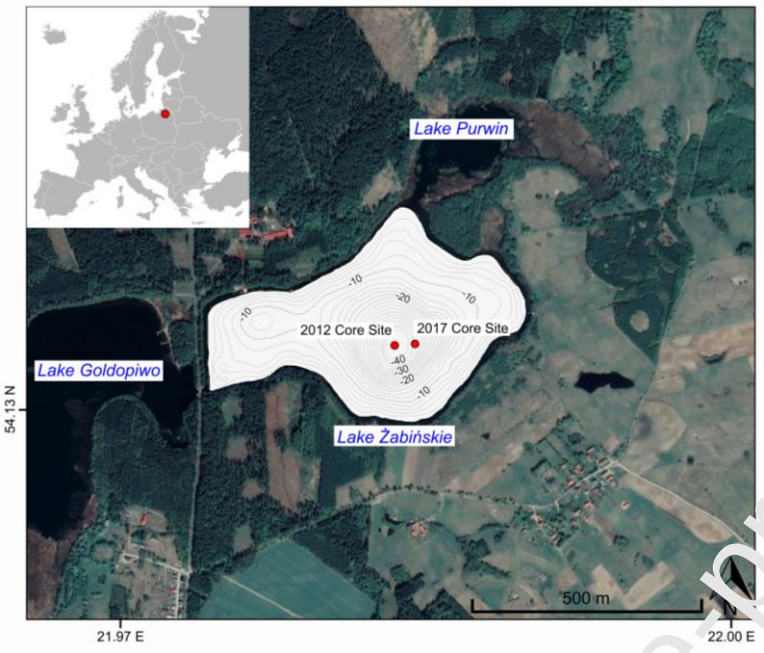


Fig. 1: Study area and bathymetric map. Imagery from Google Earth (April 29, 2019). Additional maps of catchment geology, and land cover can be found in (Bonk et al., 2015a; Wacnik et al., 2016)

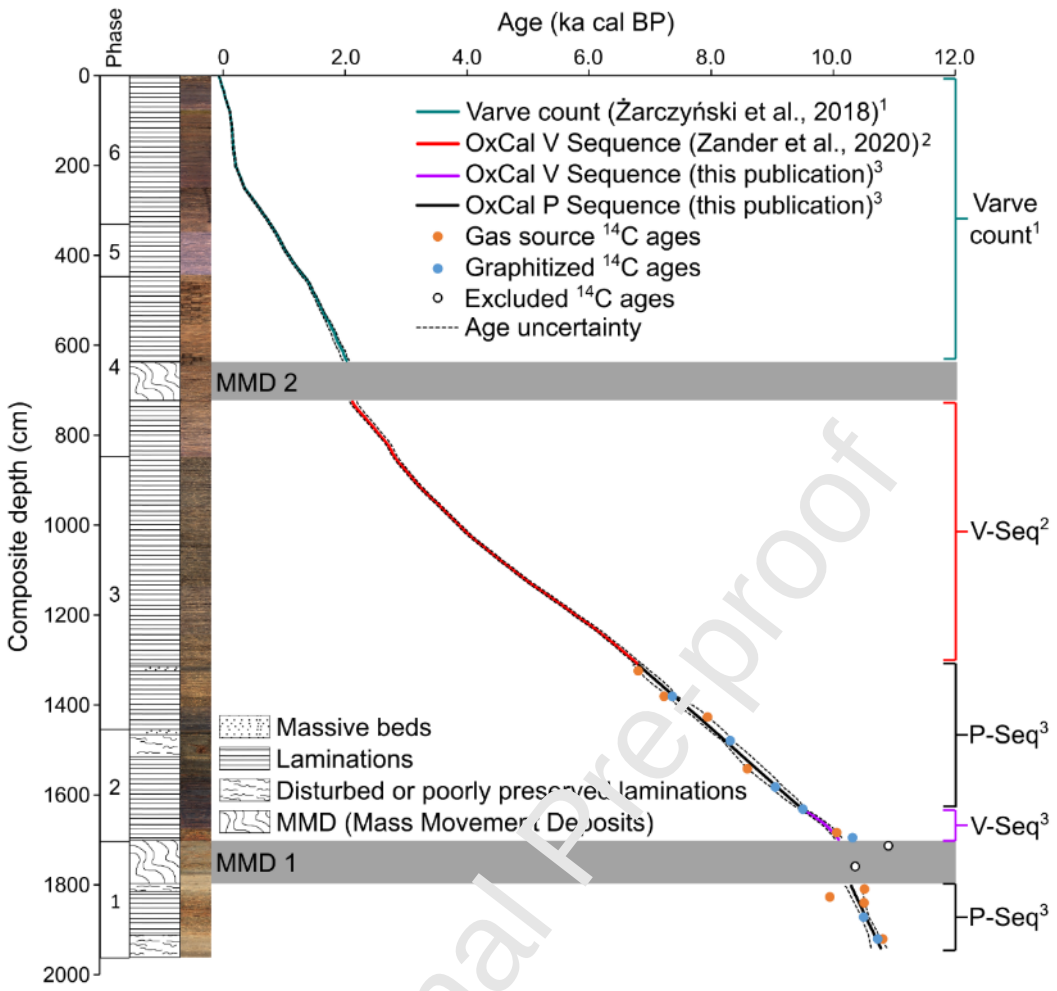


Fig. 2: Age-depth relation and core stratigraphy. Only newly reported radiocarbon ages are shown. Gas source ages contain < 150 µg C, graphitized ages contain > 150 µg C. The varve count chronology of the past 2000 years is from Żarczyński et al. (2018) and the OxCal V-sequence spanning 2.1-6.8 ka from Zander et al. (2020). The age uncertainty (dashed lines) of the varve count section was determined by comparing the counts of 3 different researchers (Żarczyński et al., 2018). For the OxCal models, the uncertainty is the 2σ range of the model output.

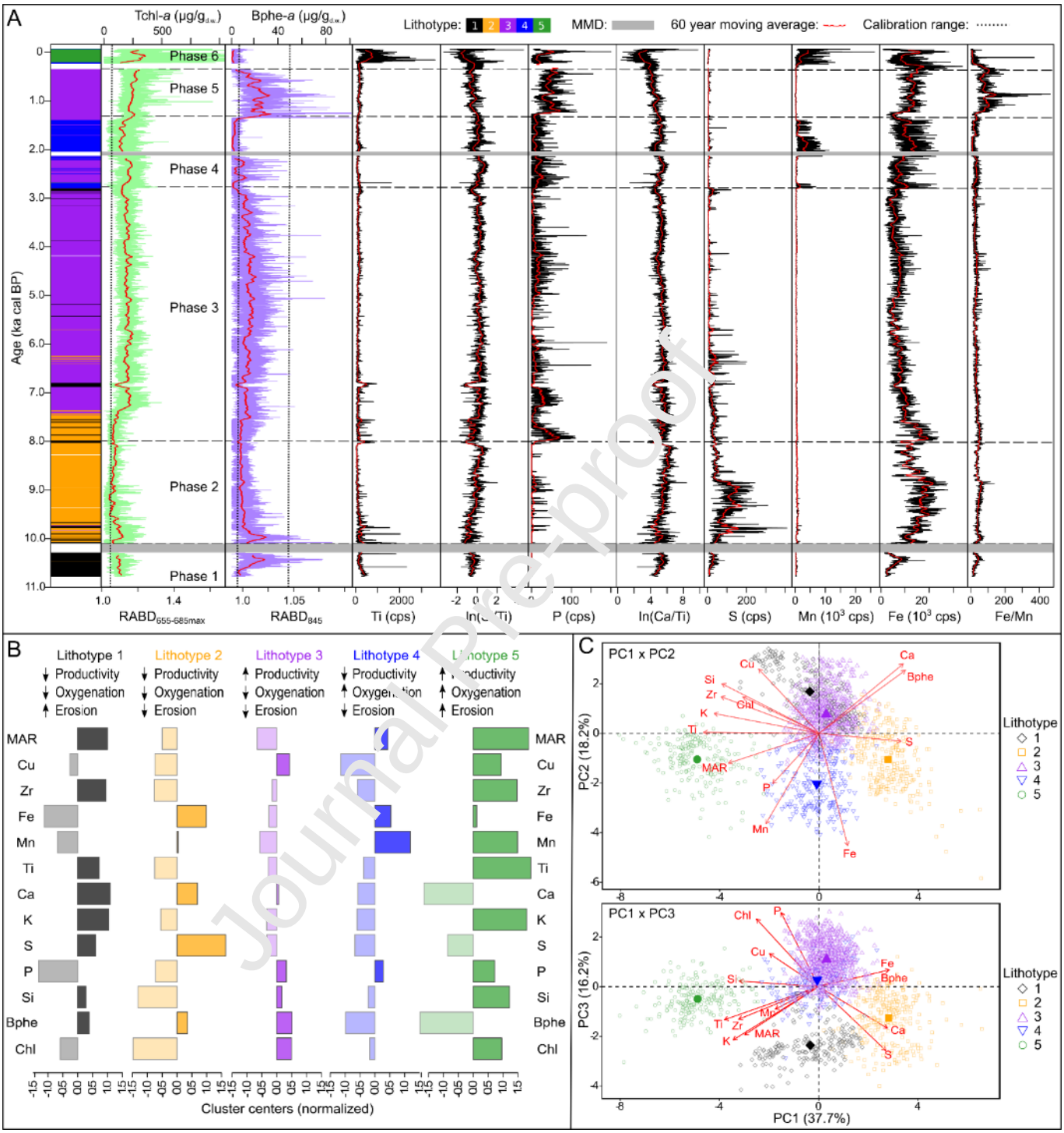


Fig. 3: A) Selected geochemical variables plotted by age. Colored bar on left shows lithotypes identified by kmeans cluster analysis. B) Cluster centers of each lithotype (normalized mean values of each geochemical variable within each lithotype). C) Principal component biplots showing first three principal components with loadings of each variable depicted as red arrows. Data points are grouped by cluster/lithotype, which is indicated by different colors and symbols, with the larger filled-in symbols representing the cluster center.

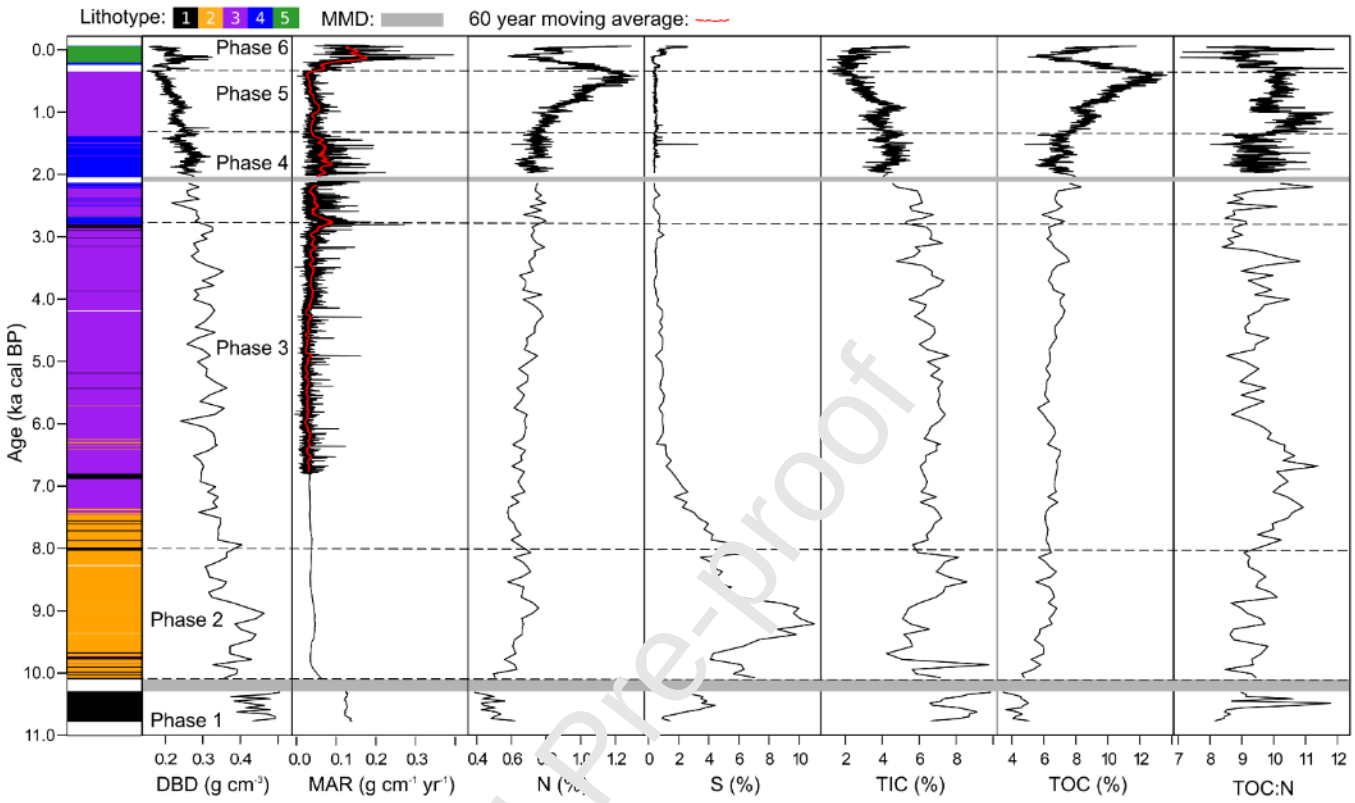


Fig. 4: Dry Bulk Density (DBD), Mass accumulation rate (MAR), and C, N, S elemental data. Red line in MAR is 60-yr average.

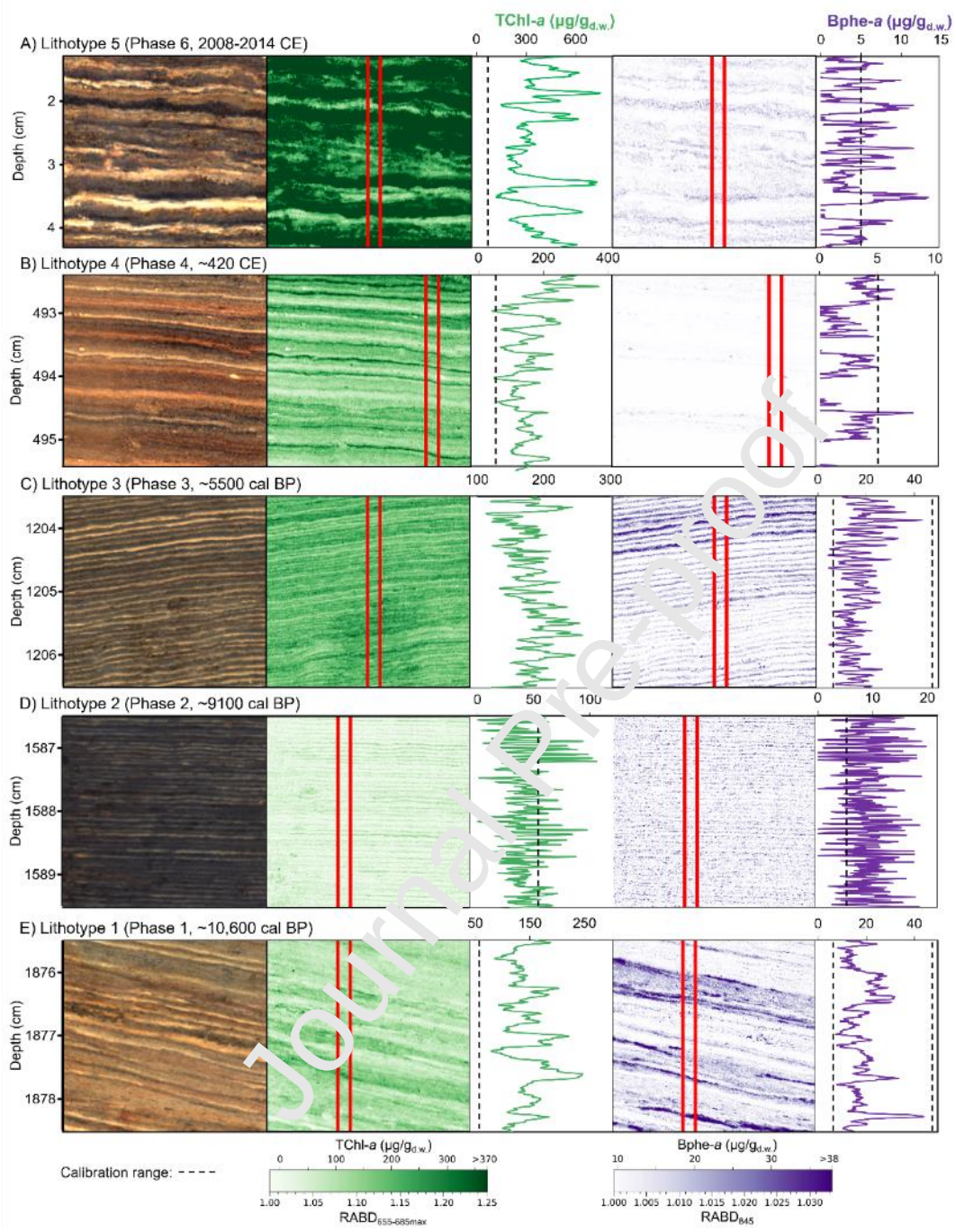


Fig. 5: Close-ups of example sections for each lithotype to show varve structure and seasonal variations of pigments detected by Hyperspectral Imaging. Each image represents 3 cm of sediments (sediment depth of composite core). Note that the axis scales change for pigment plots. A) Lithotype 5: modern sediments with high productivity and traces of Bphe-*a*. B) Lithotype 4: Fe- and Mn-rich varves during a period of more intense mixing. C) Lithotype 3: strongly stratified conditions with anoxia during the mid-Holocene. D) Lithotype 2: Dark-colored varves rich in iron-sulfides with relatively low pigment concentrations. E) Lithoytpe 1: Varves with relatively high minerogenic content, yet also Bphe-*a* present, indicating anoxia during the early Holocene.

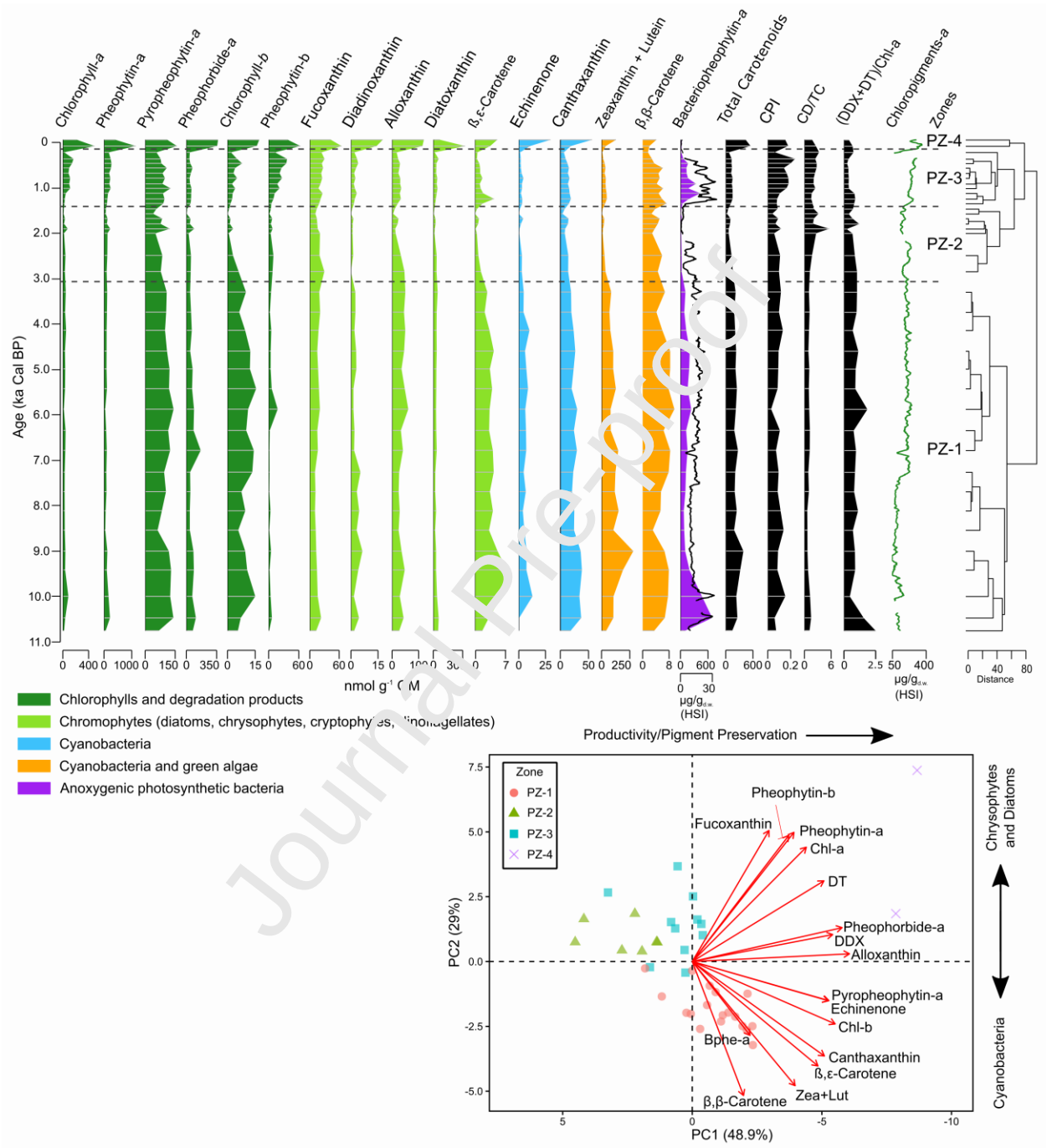


Fig. 6: HPLC pigment stratigraphy. CPI = Chlorophyll Preservation Index, TC = Total Carotenoids, DC = Chlorophyll Derivatives, DDX = Diadinoxanthin, DT= Diatoxanthin. Zones defined by CONISS analysis.

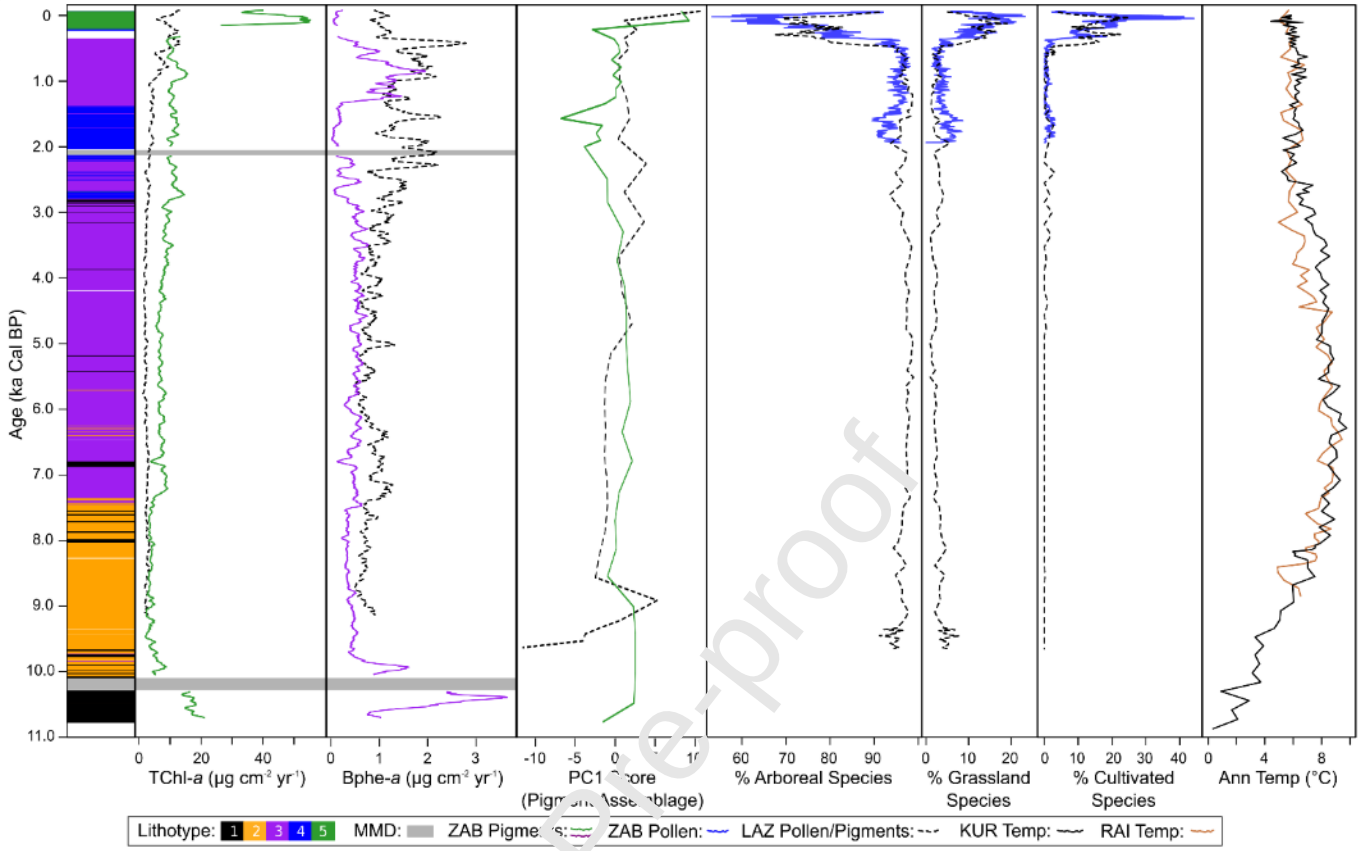


Fig. 7: Comparison of Lake Żabińskie pigment data with regional data. LAZ = Lake Łazduny data plotted as dashed black lines (Sanchini et al., 2020). KUR = Lake Kurjanovas (Heikkilä and Seppä, 2010). RAI = Lake Raigastvere (Seppä and Poska, 2004). Pigment fluxes in the first two panels are shown as 60-year running means.

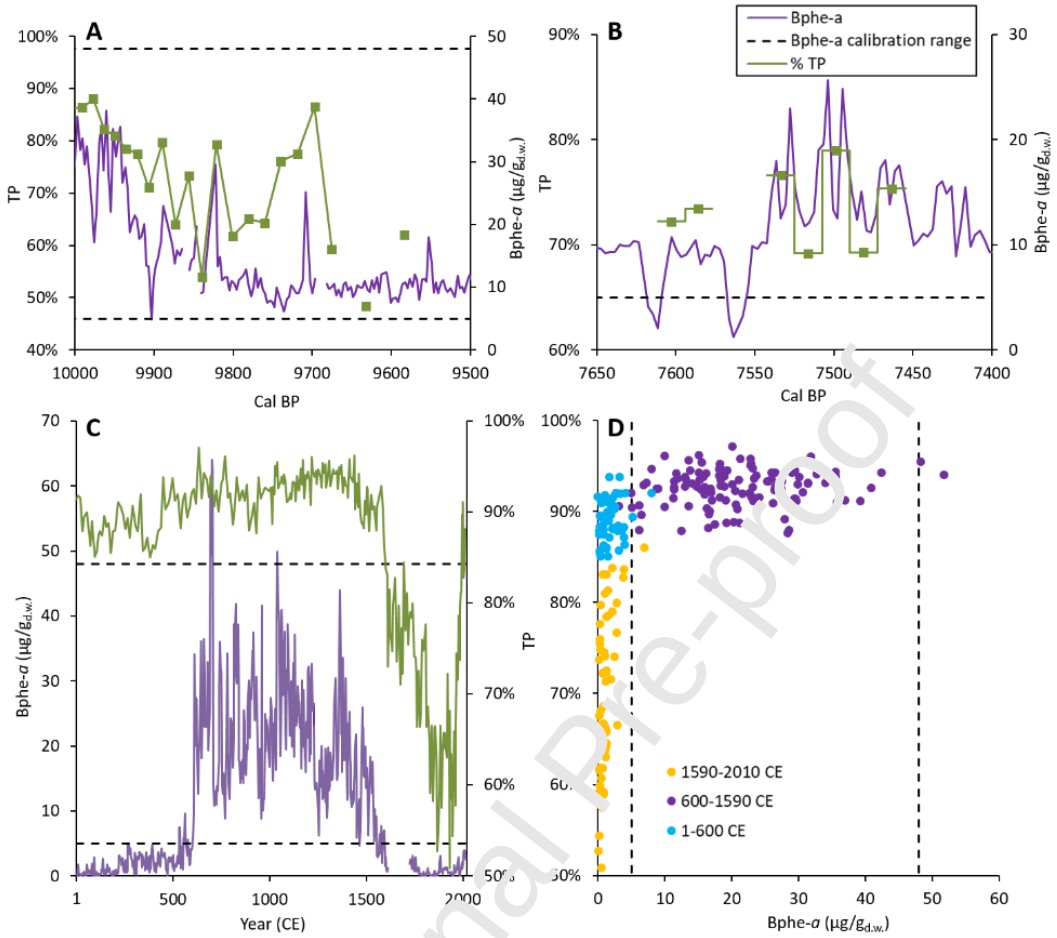


Fig. 8: A) and B): Case study comparisons of % Tree Pollen (TP) and Bphe-*a*. Bphe-*a* data is 3-year aggregate averages. C) Comparison of % TP and Bphe-*a* during past 2000 years. Bphe-*a* data is 3-year aggregate averages. D) Cross plot of Bphe-*a* and % TP during the past 2000 years, demonstrating that more anoxic conditions occurred when TP% was greater than ~90%. Note that the axis scales change for each panel. Dashed black lines represent the calibration range of Bphe-*a*.

**Declaration of interests**

☒ The authors declare that they have no known competing financial interests or personal relationships that could have appeared to influence the work reported in this paper.

☐The authors declare the following financial interests/personal relationships which may be considered as potential competing interests:

**CRediT author statement**

Paul D. Zander: Conceptualization, Formal Analysis, Investigation, Writing - Original Draft, Visualization. Maurycy Żarczyński: Investigation, Resources, Writing - Review & Editing. Hendrik Vogel: Investigation, Writing - Review & Editing. Wojciech Tylmann: Resources, Writing - Review & Editing, Project Administration, Funding Acquisition. Agnieszka Wacnik: Investigation, Writing - Review & Editing. Andrea Sanchini: Investigation, Writing - Original Draft, Visualization. Martin Grosjean: Conceptualization, Writing - Review & Editing, Project Administration, Funding Acquisition, Supervision, Resources

Graphical abstract

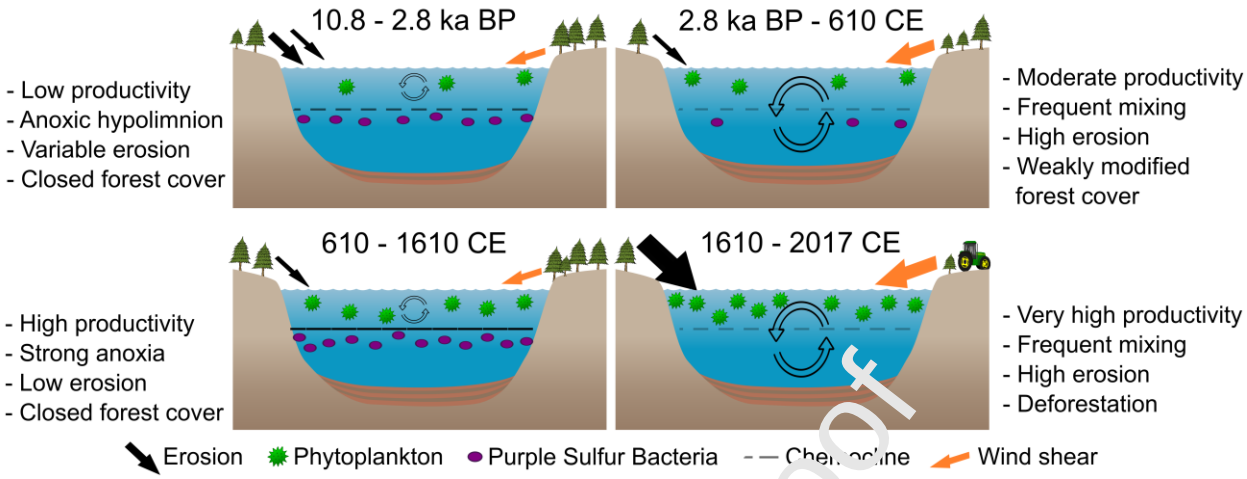

**Highlights**

- Aquatic productivity and anoxia were inferred from a 10,800-year sediment core
- Sedimentary pigments were quantified using hyperspectral imaging (HSI)
- Anoxia was persistent during the Holocene prior to human-mediated deforestation
- HSI on varves enables sub-annual reconstruction of past productivity and anoxia